

Accepted Manuscript

Green fluorescent protein chromophore derivatives as a new class of aldose reductase inhibitors

Ryota Saito, Maiko Hoshi, Akihiro Kato, Chikako Ishikawa, Toshiya Komatsu



PII: S0223-5234(16)30878-9

DOI: [10.1016/j.ejmech.2016.10.016](https://doi.org/10.1016/j.ejmech.2016.10.016)

Reference: EJMECH 8981

To appear in: *European Journal of Medicinal Chemistry*

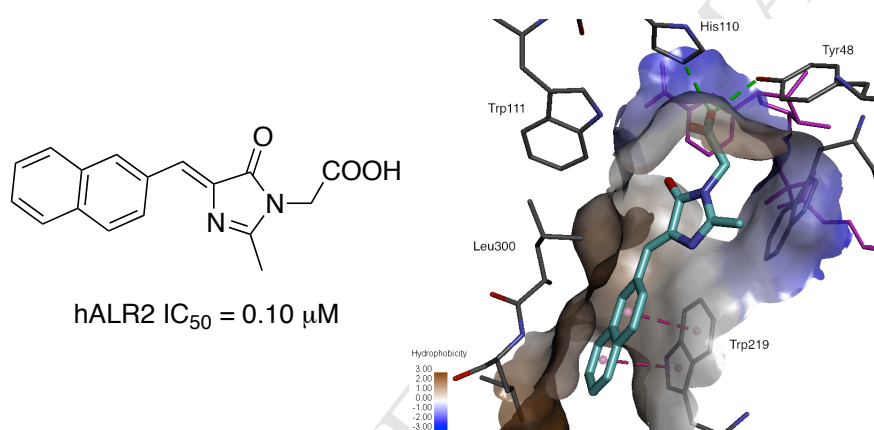
Received Date: 20 May 2016

Revised Date: 14 September 2016

Accepted Date: 7 October 2016

Please cite this article as: R. Saito, M. Hoshi, A. Kato, C. Ishikawa, T. Komatsu, Green fluorescent protein chromophore derivatives as a new class of aldose reductase inhibitors, *European Journal of Medicinal Chemistry* (2016), doi: 10.1016/j.ejmech.2016.10.016.

This is a PDF file of an unedited manuscript that has been accepted for publication. As a service to our customers we are providing this early version of the manuscript. The manuscript will undergo copyediting, typesetting, and review of the resulting proof before it is published in its final form. Please note that during the production process errors may be discovered which could affect the content, and all legal disclaimers that apply to the journal pertain.

Green fluorescent protein chromophore derivatives as a new class of aldose reductase inhibitorsRyota Saito,^{a,b*} Maiko Hoshi,^a Akihiro Kato,^a Chikako Ishikawa,^c and Toshiya Komatsu^d^aDepartment of Chemistry, Toho University, 2-2-1 Miyama, Funabashi, Chiba, 274-8510 Japan;^bResearch Center for Materials with Integrated Properties, Toho University, 2-2-1 Miyama, Funabashi, Chiba 274-8510, Japan; ^cFaculty of Pharmaceutical Science, Toho University, 2-2-1 Miyama, Funabashi, Chiba, 274-8510 Japan; ^dKowa Company, Ltd., 3-4-14 Nihonbashi-honcho, Chuo-ku, Tokyo 103-8433, Japan**Graphical Abstract**

Ryota Saito,^{a,b*} Maiko Hoshi,^a Akihiro Kato,^a Chikako Ishikawa,^c and Toshiya Komatsu^d

^aDepartment of Chemistry, Toho University, 2-2-1 Miyama, Funabashi, Chiba, 274-8510 Japan;

^bResearch Center for Materials with Integrated Properties, Toho University, 2-2-1 Miyama, Funabashi,

Chiba 274-8510, Japan; ^cFaculty of Pharmaceutical Science, Toho University, 2-2-1 Miyama, Funabashi,

Chiba, 274-8510 Japan; ^dKowa Company, Ltd., 3-4-14 Nihonbashi-honcho, Chuo-ku, Tokyo 103-8433,

Japan

Abstract. A number of (*Z*)-4-arylmethylidene-1*H*-imidazol-5(4*H*)-ones, which are related to the fluorescent chromophore of the *Aequorea* green fluorescent protein (GFP), have been synthesized and evaluated their *in vitro* inhibitory activity against recombinant human aldose reductase for the first time. The GFP chromophore model **1a**, with a *p*-hydroxy group on the 4-benzylidene and a carboxymethyl group on the N1 position, exhibited strong bioactivity with an IC₅₀ value of 0.36 μM. This efficacy is higher than that of sorbinil, a known highly potent aldose reductase inhibitor. Compound **1h**, the 2-naphthylmethylidene analogue of **1a**, exhibited the best inhibitory effect among the tested compounds with an IC₅₀ value of 0.10 μM. Structure-activity relationship studies combined with docking simulations revealed the interaction mode of the newly synthesized inhibitors toward the target protein as well as the structural features required to gain a high inhibitory activity. In conclusion, the GFP chromophore model compounds synthesized in this study have proved to be potential drugs for diabetic complications.

Keywords

Aldose reductase inhibitor; Drug candidates for diabetic complications; GFP chromophore model; (*Z*)-4-Arylmethylidene-1*H*-imidazol-5(4*H*)-ones; Docking study

1. Introduction

Aldose reductase (ALR2; EC 1.1.1.21) is an NADPH-dependent enzyme that catalyzes the reduction of D-glucose to D-sorbitol using NADPH as a reductant in the polyol pathway (Figure 1) [1, 2]. Ordinarily, most glucose is metabolized via the tricarboxylic acid (TCA) cycle in the glycolytic system. In patients with hyperglycemia, however, glucose actively fluxes not only into the glycolytic system but

also into the polyol pathway, where ALR2 is activated to consume the flooded glucose [1, 2]. Therefore, high levels of D-sorbitol are formed intracellularly. Since the oxidation of D-sorbitol to D-fructose is very slow, the intracellular concentration of D-sorbitol increases and a large amount of NADPH is consumed, resulting in an osmotic pressure imbalance that causes some diabetic complications such as peripheral neuropathy, cataract, nephropathy, and angiopathy [1, 3-8]. Hence, the inhibition of ALR2 activity may offer a promising option for the alleviation or prevention of complications and symptoms associated with chronic hyperglycemia [7, 9-11].

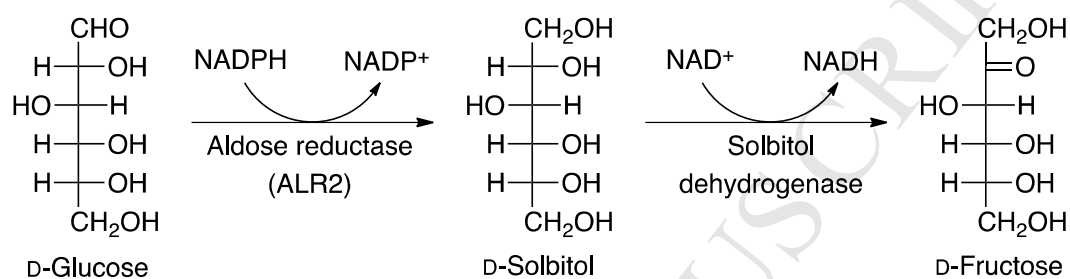


Figure 1. Schematic representation of the polyol pathway of glucose metabolism

Various types of ALR2 inhibitors (ARIs) have been reported and tested in clinical trials, but many of them presented low activity or undesirable side effects [4, 12-14]. Currently, only epalrestat (Figure 2) is launched on the market as the therapeutic medicine for diabetic peripheral neuropathy in Japan [14-17]. Owing to the limited number of drugs available for the treatment of diabetic complications, the development of new ARIs has still been strongly desired.

ARIs exhibiting strong ALR2 inhibitory effects generally fall into two structural categories; those containing an *N*-carboxymethyl (NCH₂CO₂H) moiety and those with a cyclic imide represented by a spirohydantoin or related ring system [2, 11, 13, 14, 16, 18, 19]. These acidic functional groups are believed to dissociate and form the corresponding anionic conjugate bases under physiological pH conditions to interact, through hydrogen bonds, with the catalytic site of the protein composed of Tyr48, His110, Trp20, and Trp111 side chains, adjacent to which the coenzyme NADPH is placed. The catalytic site is also called an “anion binding pocket” since His110 is positively charged under physiological pH conditions by protonation and, therefore, attracts the carbonyl oxygens of substrates, or negatively charged substituents, such as carboxylates. Adjacent to the catalytic site, ALR2 has a lipophilic pocket composed of the residues Trp20, Phe122, and Trp219, and, therefore, highly potent ARIs require having a hydrophobic moiety [2, 20-23]. Epalrestat possesses exactly these key units.

The well-known green fluorescent protein (GFP) from the jellyfish *Aequorea victoria* has a (Z)-4-(*p*-hydroxyphenylmethylene)-1*H*-imidazol-5(4*H*)-one ring system as a chromophore, formed by

autocatalytic posttranslational cyclization and oxidation of the tripeptide Ser65-Tyr66-Gly67 in the protein sequence (Figure 2) [24-27].

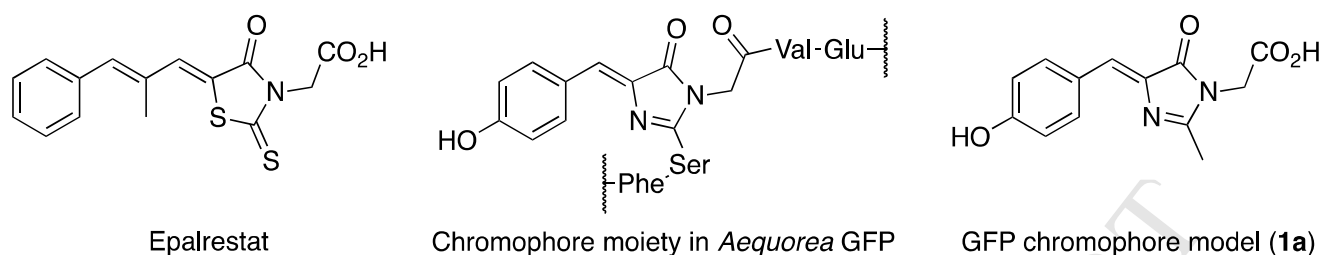


Figure 2. Structures of epalrestat, the chromophore moiety in the *Aequorea* green fluorescent protein (GFP), and the GFP chromophore model compound **1a**.

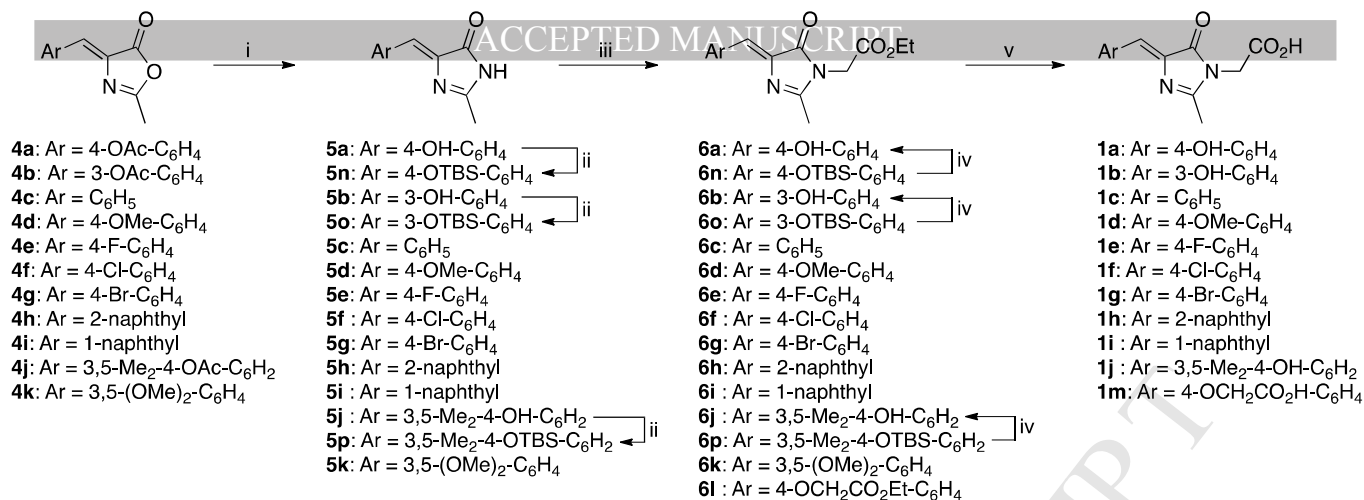
Interestingly, the GFP chromophore model structure contains the $\text{NCH}_2\text{CO}_2\text{H}$ fragment, and has a similar molecular skeleton and electronic structure to epalrestat. In spite of these features, no studies have investigated the inhibitory activity of the GFP chromophore models against ALR2 thus far.

In this study, we synthesized several GFP model compounds, evaluated their *in vitro* inhibitory activity against the recombinant human ALR2, and provided the first example of structure-activity relationship among this family of compounds.

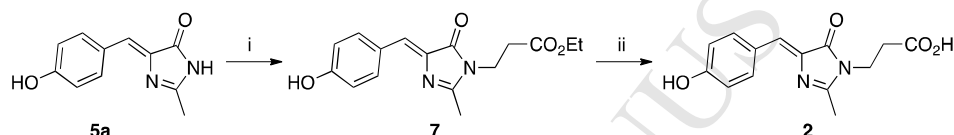
2. Results and discussion

2.1. Synthesis of (Z)-4-arylmethylene-1H-imidazol-5(4H)-ones

(Z)-4-Arylmethylidene-1H-imidazol-5(4H)-ones were synthesized using the procedure reported by Niwa *et al.*[28-30] Azlactones **4a-k** were first prepared by reacting *N*-acetylglycine with appropriate arylaldehydes in acetic anhydride in the presence of sodium acetate [28, 31-36], and afterward reacted with aqueous ammonia to give the imidazolones **5a-k** (Scheme 1). Imidazolones **5a-c**, containing hydroxy groups, were protected with *tert*-butyldimethyl silyl (TBS) groups to form **5n-p**, respectively. The obtained imidazolones **5c-i** and **5n-p** were then reacted with ethyl bromoacetate in acetone in the presence of K_2CO_3 to yield **6c-i** and **6n-p**, respectively [27]. The TBS protecting groups in **6n-p** were then removed with tetra-*n*-butylammonium fluoride (TBAF) to give the corresponding **6a-c**. Afterward, **6a-j** were hydrolyzed to give the corresponding carboxylic acids **1a-j**. The reaction of unprotected **5a** with 2 equivalents of ethyl bromoacetate yielded **6l**, which was then hydrolyzed to form compound **1m**. Compound **2**, containing the β -alanine fragment ($\text{NCH}_2\text{CH}_2\text{CO}_2\text{H}$) as a substitute of the glycine unit ($\text{NCH}_2\text{CO}_2\text{H}$) present in **1a**, was synthesized by reacting **5a** with ethyl acrylate in the presence of cesium fluoride in acetonitrile, followed by a hydrolysis of the resulting ester (Scheme 2).



Scheme 1. Reagents and conditions: (i) 28% NH₄OH, K₂CO₃, EtOH, reflux; (ii) TBSCl, imidazole, DMF, r.t.; (iii) BrCH₂CO₂Et, K₂CO₃, acetone, reflux; (iv) TBAF, MeOH, r.t.; (v) NaOH, EtOH, then H₃O⁺.



Scheme 2. Reagents and conditions: (i) CH₂=CHCO₂Et, CsF, MeCN, reflux; (ii) NaOH, EtOH, then H₃O⁺.

The structures of **1a–j**, **1m**, and **2** were assigned on the basis of their spectroscopic data. In the ¹H-NMR spectra, each compound showed a singlet peak around 6.98–7.28 ppm, assignable to the olefinic proton, which indicates that these are *cis*-isomers, while the corresponding *trans*-isomers exhibit the resonance of the olefinic protons with about 0.25-ppm higher chemical shift values [37]. X-ray crystallographic analysis of **6k**, which was prepared as depicted in Scheme 1, further confirmed the *cis* configuration: Figure 3 shows an ORTEP diagram of **6k**, clearly showing that the C=C at the C4 position of the imidazole ring takes a *cis* configuration. Unfortunately, several attempts to deprotect the methyl protecting groups in **6k** have only resulted in recovery or decomposition of the compound.

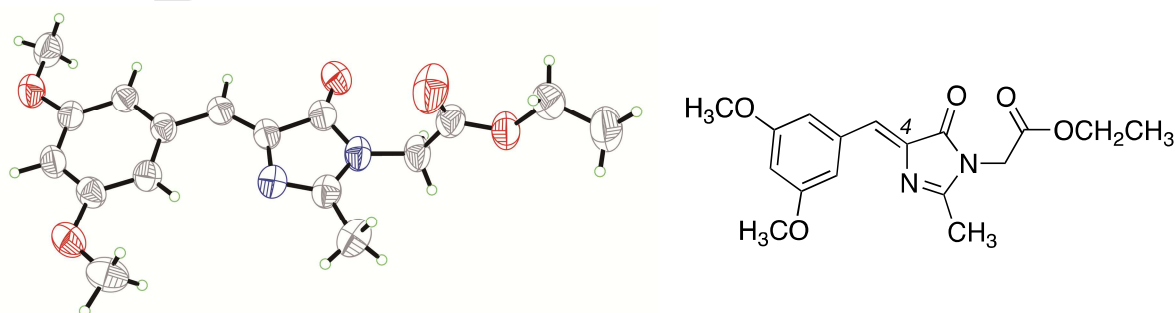
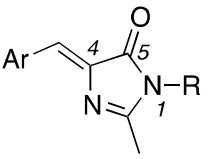


Figure 3. An ORTEP diagram of **6k**

2.2. *In vitro* aldose reductase inhibitory activity of (Z)-4-arylmethylene-1*H*-imidazol-5(4*H*)-ones

The ALR2 inhibitory activity of the synthesized imidazolones (**1a–j**, **1m**, and **2**) was evaluated *in vitro* by measuring their inhibitory effects on the reduction of D,L-glyceraldehyde with the recombinant human ALR2 in the presence of the cofactor NADPH [38–40]. The reaction was monitored with the use of a spectrophotometer by measuring NADPH consumption, as previously reported [41]. The respective IC₅₀ values, which express the 50% inhibition concentration of the compounds on the bioreduction, are shown in Table 1. The reference compound epalrestat was also assayed in the same manner, and the result is compiled in Table 1.

Table 1. *In vitro* inhibitory activity of (Z)-4-arylmethylene-1*H*-imidazol-5(4*H*)-ones **1a–j**, **1m**, **2**, **6a**, **6c**, **6f**, **6g**, **6l**, and epalrestat against recombinant human ALR2

Compound	Ar	π^a	R	IC ₅₀ (μM) ^b	
	1a	4-OH-C ₆ H ₄		CH ₂ CO ₂ H	0.36
	1b	3-OH-C ₆ H ₄		CH ₂ CO ₂ H	3.20
	1c	C ₆ H ₅	1.96	CH ₂ CO ₂ H	0.58
	1d	4-OMe-C ₆ H ₄	1.94	CH ₂ CO ₂ H	0.51
	1e	4-F-C ₆ H ₄	2.10	CH ₂ CO ₂ H	0.65
	1f	4-Cl-C ₆ H ₄	2.67	CH ₂ CO ₂ H	0.27
	1g	4-Br-C ₆ H ₄	2.82	CH ₂ CO ₂ H	0.24
	1h	2-naphthyl	3.07	CH ₂ CO ₂ H	0.10
	1i	1-naphthyl		CH ₂ CO ₂ H	0.54
	1j	3,5-diCH ₃ -4-OH-C ₆ H ₄		CH ₂ CO ₂ H	0.13
	1m	4-OCH ₂ CO ₂ H-C ₆ H ₄		CH ₂ CO ₂ H	0.31
	2	4-OH-C ₆ H ₄		(CH ₂) ₂ CO ₂ H	10.7
	6a	4-OH-C ₆ H ₄		CH ₂ CO ₂ Et	23
	6c	C ₆ H ₅		CH ₂ CO ₂ Et	112
6f	4-Cl-C ₆ H ₄		CH ₂ CO ₂ Et	16% (13 μM) ^c	
6g	4-Br-C ₆ H ₄		CH ₂ CO ₂ Et	n.d. ^d	
6l	4-OCH ₂ CO ₂ Et-C ₆ H ₄		CH ₂ CO ₂ Et	109	
epalrestat				0.085	

^a Hydrophobicity parameters of Ar groups [42, 43]. ^b 50% inhibition concentrations. ^c % inhibition at the given concentration. ^d The value could not be determined owing to the poor solubility of the test compound toward the assay medium.

The IC₅₀ value of **1a** was estimated to be 0.36 μM , indicating about 6-fold higher level of activity than sorbinil, a highly potent ARI (IC₅₀ = 0.9–20 μM against various ALR2) [22, 44, 45]. This result strongly indicates that the GFP chromophore model represents a good ARI candidate.

A closer examination of the obtained ALR2 inhibition data gives insights into several structure-activity relationship. First, the ethyl esters **6a**, **6c**, **6f**, **6g** and **6l** inhibited ALR2 less than the

corresponding carboxylic acids **1a**, **1c**, **1f**, **1g**, and **1m**, indicating that the carboxylic acid moiety is essential for the ALR2 inhibition activity as expected. Replacing the glycine unit (NCH₂CO₂H) in **1a** with the β -alanine fragment (NCH₂CH₂CO₂H), *i.e.* extending the methylene chain, resulted in a drastic decrease in the bioactivity (**2**, IC₅₀ = 10.7 μ M). These results indicate that the carboxymethyl group at the N1 position is important and that the methylene-chain length is essential for the interaction with the catalytic site of the enzyme.

Next, we examined the relationship between the structure of the arylmethylidene moiety at the C4 position and the ALR2 inhibitory activity of some of the compounds. The removal of the hydroxyl group on the phenyl ring in **1a**, resulting in compound **1c**, reduced the bioactivity (IC₅₀ = 0.58 μ M). The methyl protection of the hydroxyl group in **1a** led to the less effective derivative **1d** (IC₅₀ = 0.51 μ M). Moving the hydroxyl group of **1a** to position 3 of the 4-phenylidene ring (**1b**) markedly diminished the inhibitory activity (IC₅₀ = 3.20 μ M). In contrast, compound **1m** with a *para* carboxymethoxy group on 4-phenylidene produced almost equal inhibitory activity (IC₅₀ = 0.31 μ M) to that of **1a**. From these results, it is possible to deduce that a substituent capable of hydrogen bonding at the *para* position of the 4-phenylidene moiety may be important to achieve a significant inhibitory activity. However, a paradoxical behavior was observed with the halogenated analogues **1e–g**. The fluoro derivative **1e** was about two-fold less effective (IC₅₀ = 0.65 μ M) than **1a**, whereas the isosteric replacement of the fluorine atom in **1e** with chlorine (**1f**, IC₅₀ = 0.27 μ M) and bromine atoms (**1g**, IC₅₀ = 0.24 μ M) increased the bioactivity. Based on these observations, the effects of halogen atoms at the *para* position of the 4-phenylidene moiety on the ALR2 inhibitory activity can be ranked in the following order: of Br>Cl>F. These results give us another insight into structure-activity relationship, as the above chemical modifications decrease the molecular polarity of the compounds and increase their hydrophobicity. In fact, the hydrophobic fragmental constants for F, Cl, and Br atoms in *n*-octanol are 0.399, 0.922 and 1.131, respectively, indicating hydrophobicity in the order of Br>Cl>F [46].

Taking these factors and the above observations into account, our understanding is that chemically modifying **1a** with substituents that increase the hydrophobicity around the 4-arylmethylidene moiety results in a more profound ALR2 inhibitory activity of the GFP chromophore model family. Substituents at the *para* position of the 4-phenylidene capable of forming hydrogen bonds improve the inhibitory effect to a certain degree, but the hydrophobicity-raising modifications predominantly enhance the activity probably by increasing the affinity of this moiety toward the lipophilic pocket of the enzyme. Supplementary data supporting this consideration were obtained with **1h** and **1j**. In **1h**, the introduction of 2-naphthylmethylidene at the C4 position enhanced the inhibitory activity (IC₅₀ = 0.10

μM) to a value similar to that of the positive control epalrestat, and resulted in the best ARI for the efficacy among the tested compounds in this study. Compound **1j** has two methyl groups adjacent to the hydroxyl group exhibited 3-fold higher inhibitory activity ($\text{IC}_{50} = 0.13 \mu\text{M}$) than that of the corresponding analogue **1a**. Altering the substitution pattern in **1h** from β to α (derivative **1i**) diminished the inhibitory activity ($\text{IC}_{50} = 0.54 \mu\text{M}$). These results strongly suggest that not only the acetic acid unit at the N1 position but also an arylmethylidene fragment with increased hydrophobicity and appropriate shape to fit the lipophilic pocket (*e.g.*, the bicyclic aromatic systems), on the C4 position of the central imidazolone skeleton is favorable for improving the ALR2 inhibitory activity of the GFP model compounds.

2.3. Docking studies

In order to obtain better insight in the interactions between the imidazolones and ALR2, docking experiments were performed using known high-resolution X-ray crystal structures of the human ALR2. Nearly one hundred X-ray crystal structures of human ALR2 with various kinds of inhibitors have already been reported. Based on these experimental data, the ALR2 binding site can be divided into three sub-regions. Two of them are the catalytic and lipophilic pockets as mentioned above, while the third region is defined as a specificity pocket, and is adjacent to the other two pockets [2]. While the structure of the catalytic pocket is almost identical in the majority of the reported crystal structures, the specificity pocket has a flexible structure to accommodate various ligands. This ligand-induced-fit function is achieved by a movement of the Cys298–Cys303 loop region, and this brings two distinct states of the specificity pocket, “open” and “closed.” According to Klebe and co-workers, the ligand-binding conformations of ALR2 can be classified into five types, and these are exemplified by the PDB structures 1PWM, 1Z3N, 2FZD, 2NVC, and 2NVD [47, 48]. These structures have been frequently used in ALR2 docking studies [23, 49, 50], and were used here as well. It should be noted that none of these structures contains epalrestat as a ligand. Recently, the first report of the X-ray crystal structure of ALR2 with epalrestat (PDB ID: 4JIR) has finally been published by Zhang *et al.*, and showed that the specificity pocket is in the “closed” conformation and that the hydrophobic moiety of epalrestat is located in the lipophilic pocket [51]. Considering the structural similarities of our compounds with epalrestat, this PDB structure was also used in the present study. Here, we also include an extra ALR2 crystal structure that was very recently reported by Klebe and co-workers (PDB ID: 4IGS) [52], as the binding moiety of the ligand is a phenolic hydroxyl group, which is present in some of the imidazolones synthesized in this study. Interestingly, the protein conformation of 4IGS is almost similar to that of

1PWM except for the positions of Trp20, Phe122, and Trp219, composing the lipophilic pocket. These small changes seem to affect the docking results of our ligands since the imidazolones in this study structurally resemble epalrestat, which certainly interacts with this pocket.

The optimized structures and atom charges of the selected ligands for docking simulations were calculated by the semi-empirical PM7 calculation method with the COSMO solvation model [53-55]. The above X-ray crystal structure obtained with **6k** was adopted as the initial geometry for each ligand calculation, and the dielectric constant of water was used to calculate the properties of the ligands in water. Density Functional Theory (DFT) calculations [56, 57] were also performed at the B3LYP/6-31G(d) level [58-61] to obtain the optimized structures of the ligands, but in all cases the optimized geometries were such that the aryl group was almost planar to the exomethylene moiety. This conformation certainly gives rise to a collision between the vinyl proton and the ortho proton on the aryl group, showing that the geometries optimized by the DFT calculations are impractical. Therefore, the PM7 results were adopted for the following docking study.

All the docking experiments were performed using the GOLD Suite software package [62, 63]. ChemPLP scoring function [64] was used to predict the docking poses, and the obtained poses were rescored with Astex Statistical Potential (ASP) [65], known as a good scoring function for proteins required to make specific hydrogen bonds with ligands.[66] The best pose for each ligand was determined by considering the results obtained with both of these scoring functions (both ChemPLP and ASP give positive values, with the higher score indicating the more likely pose).

Table 2 shows the docking results of selected imidazolones (**1a-j**, **1m**, **2**, and **6a**), expressed in terms of ChemPLP fitness scores. In order to assess whether these results match the experimental data, the coefficients of determination (r^2) between these fitness scores and the pIC₅₀ values were calculated and the results are compiled in Table 2.

The docking into proteins in the “open” conformation, *i.e.* 1Z3N and 2FZD, gave relatively low fitness scores and the correlation between these scores and the pIC₅₀ values were very poor (r^2 of 0.018 and 0.143, respectively). Hence, it is possible to postulate that above compounds are not capable of opening the specificity pocket, and might better fit into a protein with the specificity pocket “closed”.

Almost all compounds showed the best fitness score with the 1PWM structure. However, some of the docking poses in 1PWM are inconsistent with the experimental results. For instance, the best score was obtained for **1h**, whose inhibitory activity was about two-fold less than that of **1i**. Moreover, compound **1b** exhibited ten-fold lower activity, but better docking score than **1a**. Furthermore, when we examined the r^2 values, the correlation between the pIC₅₀ values and the docking scores for the protein-ligand

complexes was poor for 1PWM ($r^2 = 0.367$), but, on the other hand, that was strong for 4IGS ($r^2 = 0.908$).

Table 2.^a ChemPLP fitness scores for the docking experiments with thirteen selected compounds into seven different protein structures obtained from the Protein Data Bank (PDB) compiled with the coefficients of determination (r^2) between pIC₅₀ values and ChemPLP

Compound	Protein structure (state of the specificity pocket)						
	1PWM (closed)	1Z3N (open)	2FZD (open)	2NVC (closed)	2NVD (closed)	4IGS (closed)	4JIR (closed)
1a	<i>147.9677</i>	121.0379	<i>118.4920</i>	122.6749	106.3769	132.4328	122.4033
1b	148.8442	116.7325	122.4086	<i>132.3547</i>	110.9174	127.3476	118.8936
1c	146.4784	120.4499	119.1567	123.3144	106.6123	131.2452	122.7660
1d	149.7175	123.0365	117.1841	126.5613	107.9176	134.6136	123.0212
1e	148.6791	122.3372	116.6743	124.8679	106.1159	136.5031	122.2602
1f	148.3229	122.1758	116.4419	126.7387	106.9029	136.0539	123.6788
1g	148.3499	121.7783	116.4413	126.0770	106.8894	135.7583	123.7556
1h	163.8831	125.6343	125.1224	135.8675	112.0374	145.9120	128.9951
1i	167.0596	126.2255	123.2132	143.3077	114.4054	135.9552	129.1376
1j	159.7231	123.7278	118.3947	132.4810	112.8971	142.0384	128.7544
1m	153.6158	120.0431	119.0217	<i>136.7273</i>	109.7848	<i>135.6587</i>	124.9088
2	138.4267	134.5372	<i>118.1440</i>	<i>129.4450</i>	96.3939	<i>121.5386</i>	119.7465
6a	<i>145.5941</i>	113.2006	<i>113.0078</i>	<i>119.7632</i>	102.9124	<i>118.6954</i>	<i>112.2170</i>
r^2	0.367	0.018	0.143	0.112	0.436	0.908	0.749
r^2 (flexible) ^b	0.038	0.385	0.143	0.270	0.319	0.211	<0.001

^a Values for ligands that were docked into the binding site of the protein with a “flipped” conformation are written in *italics*. ^b Coefficients of determination between the ChemPLP docking scores obtained by flexible docking simulations and the experimental pIC₅₀ values.

Closer examination of the docking poses for compounds **1a** and **1c–j**, which exhibited sub-micromolar IC₅₀ values, revealed that the orientation of the carboxylates at the N1 position obtained with the 4IGS structure were different from those obtained with the 1PWM. In both structures, one carboxylate oxygen atom forms a hydrogen bond with His110; the other one, however, is orientated toward Trp111 (in 4IGS) or toward Trp20 (in 1PWM), as exemplified by **1c** in Figure 4. We then consulted the Protein Data Bank (PDB) and found 31 ALR2 X-ray crystal structures, in which carboxylate-type ligands are incorporated. When we compared the predicted carboxylate orientations of our compounds to those observed in the PDB database, we found that the poses of the carboxylate groups obtained for 4IGS structure are similar to those predominantly found in the experimental crystal structures. It is therefore conceivable that the docking poses calculated using the 1PWM structure are inadequate to explain the experimental data and the docking poses with the 4IGS structure are indeed

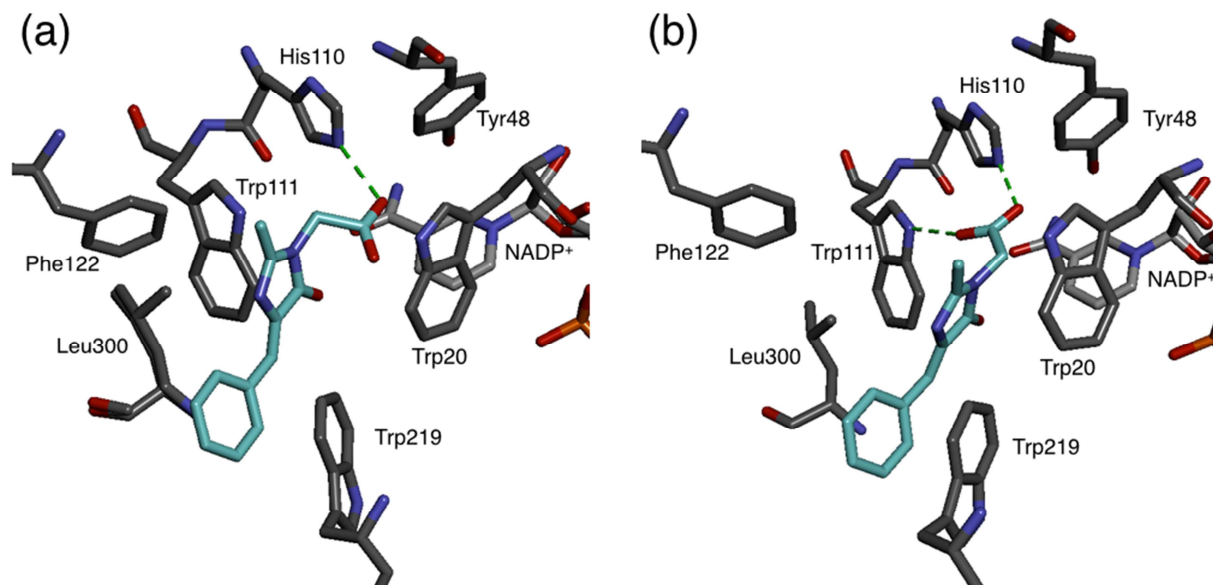


Figure 4. Depiction of the predicted binding modes for **1a** and **1c–j** docked into (a) 1PWM and (b) 4IGS exemplified by **1c**. Graphics were created by the Discovery Studio Visualizer.[67]

Further inspection of the docking poses for **1a** and **1c–j** in 4IGS revealed that all of these poses superimpose well with each other, except for **1i**, and the 4-arylidene scaffolds are placed parallel to Trp219, forming π - π interactions (Figure 5). Among these compounds, the most potent **1h** shows the best overlap between the naphthyl residue and the indole ring of Trp219. These results suggest that the hydrophobic interaction of the aromatic rings with Trp219, as well as the hydrogen-bonding interactions in the anion-binding pocket, plays an important role in ligands binding to ALR2 described in the present study. The aforementioned interactions for **1h** have been visualized using the Discovery Studio Visualizer program [67] as shown in Figure 6. The program detects a hydrogen-bond donor region in the protein close to the carboxylate group of **1h**, an aromatic face-to-face interaction region around the Trp219, and a lipophilic contact around Leu300 near the naphthyl residue of **1h**.

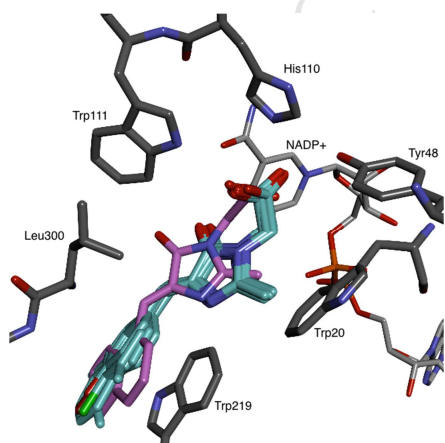


Figure 5. Superposition of the predicted docking poses for **1a** and **1c–j** docked into the binding site of 4IGS. All ligands are colored in cyan except **1i** in magenta.

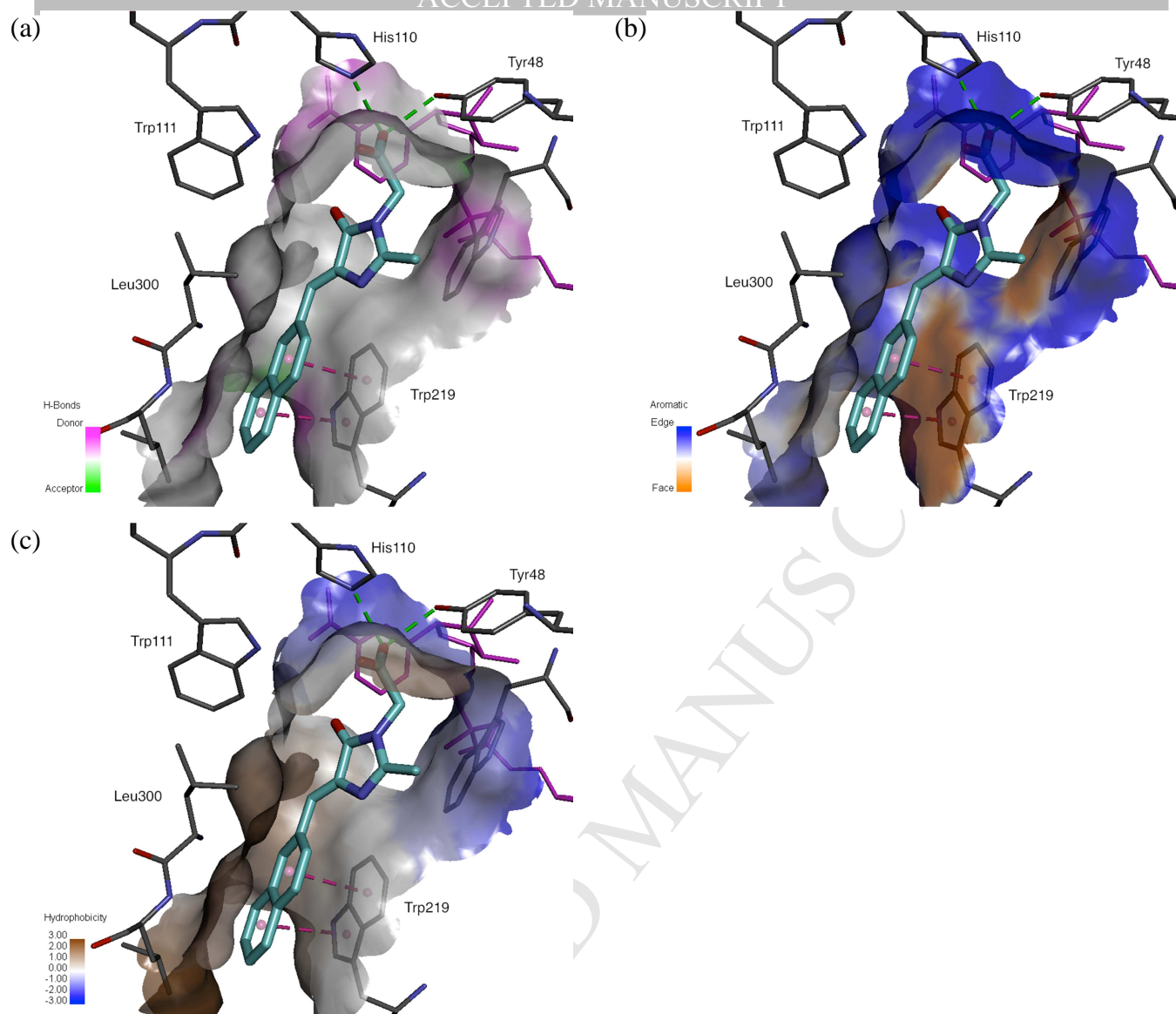


Figure 6. The contour maps of (a) hydrogen-bonding, (b) aromatic, and (c) hydrophobic interaction surfaces of the binding-site residues in 4IGS superposed with the predicted docking pose for compound **1h**. All surfaces were detected and visualized by the Discovery Studio Visualizer [67].

The program SuperStar, which empirically generates interaction maps within protein binding sites based on experimental crystal structure databases such as the Cambridge Structural Database (CSD) and PDB [68-70], was used to visualize the knowledge-based protein-ligand interaction area within the active site of 4IGS. Figure 7 depicts the PDB-based SuperStar propensity maps of the 4IGS binding site, in which the hydrophobic interaction area (magenta) was detected using the aliphatic CH probe and the hydrogen-bonding donor region (yellow) was simulated with the C=O probe. Overlapping the predicted docking pose of **1h** into this figure clearly shows that the carboxylate group and the naphthyl ring in the ligand correlates well with the areas of predicted interaction propensity. Based on these observations, the inhibitory activity of **1c-h**, whose docking modes are quite similar and superimposable to each other, is likely to vary because of difference in the degree of lipophilic contact between the aryl moiety and the

enzyme hydrophobic pocket (Trp219 and Leu300). In order to assess this consideration quantitatively, the correlation between the pIC₅₀ values and the hydrophobicity parameter for the aryl groups of **1c–h** (π) was examined, and the following equation was obtained with a high correlation coefficient.

$$\text{pIC}_{50} = 5.062 + 0.589 \pi \quad (r^2 = 0.900) \quad (1)$$

This result clearly demonstrates that the experimental inhibitory activity of **1c–h** can be described by the hydrophobicity of the 4-arylidene moiety. There might be a criticism that the biggest term in this equation is the constant value. As for this point, there have been some quantitative structure-activity relationship (QSAR) models for aldose reductase inhibitors reported with larger constant values than that in the equation 1. For example, Soni and Kaskhedikar reported a QSAR model for 2,4-dioxo-5-(naphtha-2-ylmethylene)-3-thiazolidinyl acetic acids and 2-thioxo analogues as follows:

$$\text{pIC}_{50} = 6.634 + 0.504 \Sigma\pi + 0.659 I_x \quad (r^2 = 0.726)$$

where $\Sigma\pi$ represents the sum of hydrophobicity of the substituents on the naphthyl group and I_x is the indicator variable for the presence of sulfur atom on the C2 position [71]. More recently, Nantasenamat *et al.* reported a QSAR model with a much larger constant value (6.766) and much smaller coefficients of explanatory variables (0.097–0.332) to predict aldose reductase inhibitory activity of sulfonylpyridazinones [72]. Thus one can safely say that the equation 1 is reasonable.

Compound **1a** was excluded from this assessment because an additional and hydrogen-bonding interaction with the backbone NH of Leu301 was predicted in addition to the interactions with the anion binding site and Trp219. This additional interaction is likely to raise the bioactivity, as discussed above.

The 1-naphthyl group of **1i** also faces to Trp219, but the area forming the π - π interaction is smaller than that of **1h** and similar to that of **1b**. Moreover, because of its shape, the position of **1i** within the protein slightly deviates from those of the other derivatives. These might be the reasons behind the low activity of **1i**.

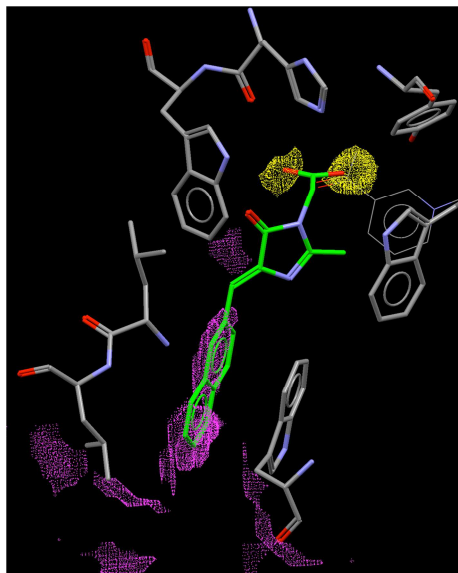


Figure 7. PDB-based SuperStar propensity map of the 4IGS binding site using the aliphatic CH (magenta) and C=O (yellow) probes accompanied with the predicted docking pose of **1h**.

The docking pose of the ester **6a**, which exhibited about 60-times less activity ($IC_{50} = 23 \mu\text{M}$) than the corresponding carboxylic acid **1a** ($IC_{50} = 0.36 \mu\text{M}$), with 4IGS was quite different from those of **1c–j**. The orientation of the imidazolone and phenyl rings is also flipped in comparison to the ones of **1c–j**, and the phenolic hydroxyl group is placed in the anion-binding pocket to form a hydrogen bond with His110 (Figure 8a). A similar “flipped” pose was obtained for compound **2** ($IC_{50} = 10.7 \mu\text{M}$), which exhibits low inhibitory activity despite the presence of a carboxyl group. As shown in Figure 8b, the anionic carboxylate group in **2** does not bind to the catalytic pocket of 4IGS, but instead makes a hydrogen bond with the backbone NH of Ser302. In contrast, the phenol moiety of **2** is inserted into the anion-binding pocket and forms a hydrogen bond with His110, the carbonyl group at the C5 position of the imidazolone ring forms a hydrogen bond with the backbone NH of Leu300, and the imidazolone ring faces to Trp219. It is conceivable that these additional interactions in part improve the bioactivity of **2** compared to that of **6a**, but its inhibitory effect is still lower than those of the carboxylic acid series **1**, probably because of the loss of the tight binding of the carboxylate with the catalytic pocket. The docking pose for **1m** in 4IGS was also solved as the “flipped” one (Figure 8c). In this pose, the carboxylate group of the glycine unit at the N1 position of the imidazolone ring points toward the outside of the protein, but instead the other carboxylate group at the *para* position of the phenyl ring forms a tight net of hydrogen bonds with Tyr48, His110 and Trp111 (the anion-binding site), providing a possible explanation for its good efficacy ($IC_{50} = 0.31 \mu\text{M}$).

For what concerns compound **1b**, a *meta* analogue of **1a**, we found a pose in which the carboxyl group was incorporated into the catalytic pocket through a hydrogen bond with His110, and the

meta-hydroxyl group formed hydrogen bonds with the backbone NH of Ala299 and Leu300 (Figure 8d). However, the entire pose was not superimposable with those obtained for **1c–j**. The amide carbonyl group at the C5 positions of the imidazolone ring in **1b** was flipped compared to **1c–j**, and thus, the hydrogen bond with Cys298, commonly observed in the poses of **1c–j**, was lost (Figure S1). Moreover, the predicted conformation of **1b** in 4IGS was not identical to the optimized geometry (Figure S2), namely the phenyl ring was rotated almost 180° in the docking experiments. According to a simple molecular mechanics calculation, the rotation barrier was estimated to be 2.0 kcal/mol, showing that extra energy is required for **1b** to be incorporated into the binding site with this particular pose. These results suggest that the binding of **1b** with the protein is energetically unfavorable compared to the others of series **1**, and this may explain the low activity of **1b**.

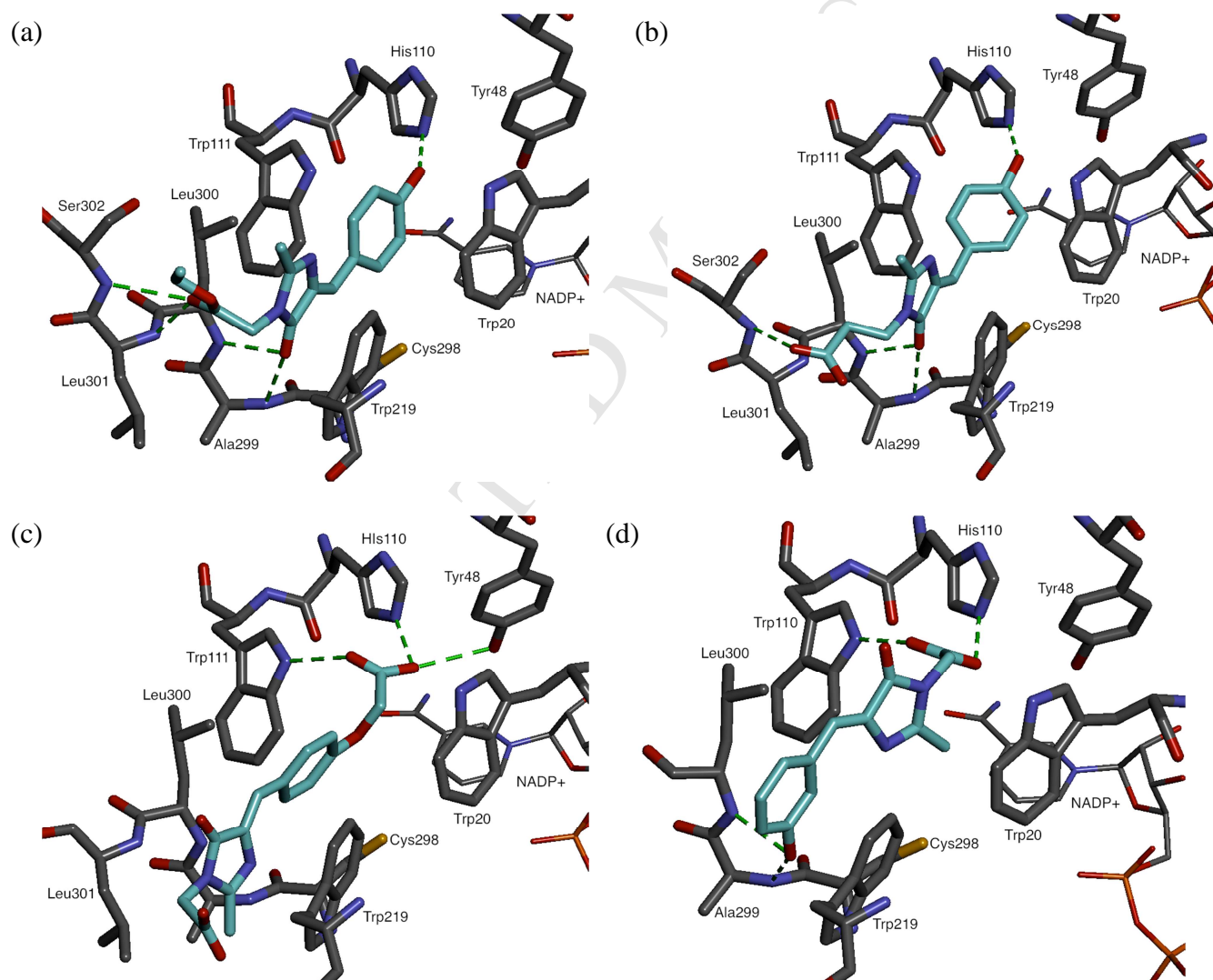


Figure 8. Predicted binding modes for (a) **6a**, (b) **2**, (c) **1m**, and (d) **1b** docked into 4IGS. Graphics were created by the Discovery Studio Visualizer [67].

Since the ALR2 binding site shows a high degree of flexibility to incorporate diverse structures of carbonyl substrates, we also performed induced-fit docking simulations [23, 73, 74] using the Side

Chain Flexibility function in GOLD. The same five protein structures described in Table 2 were used. The results indicate that the docking scores were not drastically improved, and that the correlation between the docking scores and pIC₅₀ values was poor ($r^2 < 0.4$) in all cases (Table 2). This result suggests that the predicted docking poses using the 4IGS structure with no side chains flexibility account for the present experimental results best.

By considering all these data, we conclude that correlating the docking results with the experimental IC₅₀ values is a valid approach.

3. Conclusion

We have demonstrated that some (Z)-4-Arylmethylene-1H-imidazol-5(4H)-ones related to the GFP chromophore act as good ARIs with the IC₅₀ values less than 0.36 μ M. Among these new GFP chromophore models, **1h** exhibited the best inhibitory activity with an IC₅₀ of 0.10 μ M, supporting further work on evaluating its *in vivo* efficacy. The structure-activity relationship study indicated the important structural features needed to the GFP chromophore model series to exhibit high ALR2 inhibitory activity. These include the carboxylate group at the N1 position and the hydrophobicity of the 4-arylmethylidene moiety.

We have explored a way to obtain reliable docking results by correlating the docking scores with the IC₅₀ values. In our docking study, the obtained docking poses for the imidazolones in the 1PWM structure gave the best fitness scores, but exhibited poor correlation with the efficacy of the ligands. The docking scores obtained using the 4IGS structure, on the other hand, correlated well with the experimental inhibitory activity. The predicted docking poses with 4IGS suggest that the 4-arylmethylidene moiety forms a π - π interaction with the Trp219 residue as well as lipophilic contact with Leu300, rationally explaining the importance of the hydrophobicity. In fact, a linear correlation was observed between the hydrophobicity of the 4-arylmethylidene moiety and the experimental inhibitory activity.

Some reports claimed the usefulness of induced-fit docking (IFD) methods to simulate the induced-fit-type movement of the binding site of ALR2 in accommodating substrates with diverse structures [23, 74]. Although this approach seems to be rational for modeling the complex of inhibitors with the induced-fit-type protein, none of the examples demonstrated a correlation between the docking scores and the experimental inhibitory activity in a quantitative fashion. In our system, the IFD simulation did not yield any satisfactory results that would rationally explain the experimental data, while the fully knowledge-based docking method in which the experimentally obtained protein

structures with different active site conformation were used, yielded scores and poses that accounted for the experimental results.

By considering these results comprehensively, we conclude that it is advisable to correlate between the docking results with the experimental IC₅₀ values quantitatively, in order to gain reliable information of ligand-protein interactions, independently of the docking method used.

Acknowledgement

This research was supported by a Grant-in-Aid for Scientific Research C (No. 25410179) from the Japan Society for the Promotion of Science (JSPS). Partial financial support to R.S. by the Nukada Memorial Scholarship Fund of Toho University is also gratefully appreciated. The authors thank Dr. Yoichi Habata and Dr. Shunsuke Kuwahara for carrying out the X-ray diffraction experiment and refinement of the data.

Conflicts of interest

The authors declare no other conflicts of interest.

Appendix. Supplementary data

Supplementary data related to this article can be found at <http://dx.doi.org/10.1016/j.ejmech.xxxx.xx.xxx>

References

- [1] M. Brownlee, Biochemistry and molecular cell biology of diabetic complications, *Nature* 414 (2001) 813–820.
- [2] Z. Changjin, Aldose reductase inhibitors as potential therapeutic drugs of diabetic complications, in: O. Oguntibeju (Ed.), *Diabetes mellitus - Insights and perspectives*, InTech, 2013, pp. 17–46.
- [3] K.H. Gabbay, N. Spack, S. Loo, H.J. Hirsch, A.A. Ackil, Aldose reductase inhibition: Studies with alrestatin, *Metabolism* 28 (1979) 471–476.
- [4] P.F. Kador, J.H. Kinoshita, N.E. Sharpless, Aldose reductase inhibitors - A potential new class of agents for the pharmacological control of certain diabetic complications, *J. Med. Chem.* 28 (1985) 841–849.
- [5] D. Dvornik, D. Porte, Aldose reductase inhibition: An approach to the prevention of diabetic complications, Biomedical Information Corp., 1987.
- [6] T. Tanimoto, K. Maekawa, S. Okada, C. Yabe-Nishimura, Clinical analysis of aldose reductase for differential diagnosis of the pathogenesis of diabetic complication, *Anal. Chim. Acta* 365 (1998) 285–292.
- [7] N. Hotta, T. Toyota, K. Matsuoka, Y. Shigeta, R. Kikkawa, T. Kaneko, A. Takahashi, K. Sugimura, Y. Koike, J. Ishii, N. Sakamoto, S.D.N.S. Group, Clinical efficacy of fidarestat, a novel aldose reductase

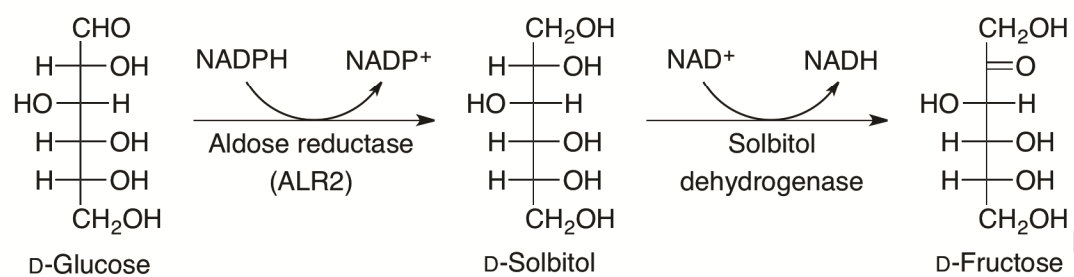
- inhibitor, for diabetic peripheral neuropathy - A 52-week multicenter placebo-controlled double-blind parallel group study, *Diabetes Care* 24 (2001) 1776–1782.
- [8] M. Lorenzi, The polyol pathway as a mechanism for diabetic retinopathy: Attractive, elusive, and resilient, *Exp. Diabetes Res.* (2007) Article ID 61038, 61010 pages. DOI:10.1155/2007/61038.
- [9] N. Hotta, New approaches for treatment in diabetes: Aldose reductase inhibitors, *Biomed. Pharmacother.* 49 (1995) 232–243.
- [10] C. Yabe-Nishimura, Aldose reductase in glucose toxicity: A potential target for the prevention of diabetic complications, *Pharmacol. Rev.* 50 (1998) 21–33.
- [11] L. Costantino, G. Rastelli, P. Vianello, G. Cignarella, D. Barlocco, Diabetic complications and their potential prevention: Aldose reductase inhibition and other approaches, *Med. Res. Rev.* 19 (1999) 3–23.
- [12] M.A. Pfeifer, M.P. Schumer, Clinical-trials of diabetic neuropathy - Past, present, and future, *Diabetes* 44 (1995) 1355–1361.
- [13] L. Costantino, G. Rastelli, G. Cignarella, P. Vianello, D. Barlocco, New aldose reductase inhibitors as potential agents for the prevention of long-term diabetic complications, *Expert Opin. Ther. Pat.* 7 (1997) 843–858.
- [14] L. Costantino, G. Rastelli, M.C. Gamberini, D. Barlocco, Pharmacological approaches to the treatment of diabetic complications, *Expert Opin. Ther. Pat.* 10 (2000) 1245–1262.
- [15] N. Hotta, N. Sakamoto, Y. Shigeta, R. Kikkawa, Y. Goto, Clinical investigation of epalrestat, an aldose reductase inhibitor, on diabetic neuropathy in japan: Multicenter study (reprinted from *excerpta medica international congress, series 1084, 1995*), *J. Diabetes Complicat.* 10 (1996) 168–172.
- [16] S. Miyamoto, Recent advances in aldose reductase inhibitors: Potential agents for the treatment of diabetic complications, *Expert Opin. Ther. Pat.* 12 (2002) 621–631.
- [17] M.A. Ramirez, N.L. Borja, Epalrestat: An aldose reductase inhibitor for the treatment of diabetic neuropathy, *Pharmacotherapy* 28 (2008) 646–655.
- [18] A. Ishii, T. Kotani, Y. Nagaki, Y. Shibayama, Y. Toyomaki, N. Okukado, K. Ienaga, K. Okamoto, Highly selective aldose reductase inhibitors. 1. 3-(arylalkyl)-2,4,5-trioxoimidazolidine-1-acetic acids, *J. Med. Chem.* 39 (1996) 1924–1927.
- [19] T. Negoro, P. Murata, S. Ueda, B. Fujitani, Y. Ono, A. Kuromiya, M. Komiya, K. Suzuki, J. Matsumoto, Novel, highly potent aldose reductase inhibitors: (*R*)-(-)-2-(4-bromo-2-fluorobenzyl)-1,2,3,4-tetrahydropyrrolo[1,2- α]pyrazine-4-spiro-3'-pyrrolidine-1,2', 3,5'-tetrone (as-3201) and its congeners, *J. Med. Chem.* 41 (1998) 4118–4129.
- [20] G. Rastelli, P. Vianello, D. Barlocco, L. Costantino, A. DelCorso, U. Mura, Structure-based design of an inhibitor modeled at the substrate active site of aldose reductase, *Bioorg. Med. Chem. Lett.* 7 (1997) 1897–1902.
- [21] M. Oka, Y. Matsumoto, S. Sugiyama, N. Tsuruta, M. Matsushima, A potent aldose reductase inhibitor, (2*S*,4*S*)-6-fluoro-2',5'-dioxospiro[chroman-4,4'-imidazolidine]-2-carboxamide (fidarestat): Its absolute configuration and interactions with the aldose reductase by x-ray crystallography, *J. Med. Chem.* 43 (2000) 2479–2483.
- [22] S. Miyamoto, Molecular modeling and structure-based drug discovery studies of aldose reductase inhibitors, *Chem-Bio Inform. J.* 2 (2002) 74–85.
- [23] R. Maccari, R. Ottana, R. Ciurleo, D. Rakowitz, B. Matuszczak, C. Laggner, T. Langer, Synthesis, induced-fit docking investigations, and in vitro aldose reductase inhibitory activity of non-carboxylic acid containing 2,4-thiazolidinedione derivatives, *Bioorg. Med. Chem.* 16 (2008) 5840–5852.
- [24] H. Morise, O. Shimomura, F.H. Johnson, J. Winant, Intermolecular energy-transfer in bioluminescent system of *aequorea*, *Biochemistry* 13 (1974) 2656–2662.
- [25] O. Shimomura, Structure of the chromophore of *aequorea* green fluorescent protein, *Febs Lett.* 104 (1979) 220–222.

- [26] C.W. Cody, D.C. Prasher, W.M. Westler, F.G. Prendergast, W.W. Ward, Chemical-structure of the hexapeptide chromophore of the aequorea green-fluorescent protein, *Biochemistry* 32 (1993) 1212–1218.
- [27] H. Niwa, S. Inouye, T. Hirano, T. Matsuno, S. Kojima, M. Kubota, M. Ohashi, F.I. Tsuji, Chemical nature of the light emitter of the aequorea green fluorescent protein, *Proc. Natl. Acad. Sci. U.S.A.* 93 (1996) 13617–13622.
- [28] S. Kojima, H. Ohkawa, T. Hirano, S. Maki, H. Niwa, M. Ohashi, S. Inouye, F.I. Tsuji, Fluorescent properties of model chromophores of tyrosine-66 substituted mutants of aequorea green fluorescent protein (GFP), *Tetrahedron Lett.* 39 (1998) 5239–5242.
- [29] P. Busca, F. Paradisi, E. Moynihan, A.R. Maguire, P.C. Engel, Enantioselective synthesis of non-natural amino acids using phenylalanine dehydrogenases modified by site-directed mutagenesis, *Org. Biomol. Chem.* 2 (2004) 2684–2691.
- [30] K.M. Khan, U.R. Mughal, M.T.H. Khan, U. Zia, S. Perveen, M. Iqbal Choudhary, Oxazolones: New tyrosinase inhibitors; synthesis and their structure–activity relationships, *Bioorg. Med. Chem.* 14 (2006) 6027–6033.
- [31] H.N.C. Wong, Z.L. Xu, H.M. Chang, C.M. Lee, A modified synthesis of (\pm)- β -aryllactic acids, *Synthesis* 1992 (1992) 793–797.
- [32] H. Hoshina, H. Tsuru, K. Kubo, T. Igarashi, T. Sakurai, Formation of isoquinoline derivatives by the irradiation of *N*-acetyl- α -dehydrophenylalanine ethyl ester and its derivatives, *Heterocycles* 53 (2000) 2261–2274.
- [33] K. Takrouri, T. Chen, E. Papadopoulos, R. Sahoo, E. Kabha, H. Chen, S. Cantel, G. Wagner, J.A. Halperin, B.H. Aktas, M. Chorev, Structure–activity relationship study of 4EGI-1, small molecule eIF4E/eIF4G protein–protein interaction inhibitors, *Eur. J. Med. Chem.* 77 (2014) 361–377.
- [34] M. Blanco-Lomas, I. Funes-Ardoiz, P.J. Campos, D. Sampedro, Oxazolone-based photoswitches: Synthesis and properties, *Eur. J. Org. Chem.* 2013 (2013) 6611–6618.
- [35] K. Maekawa, T. Igarashi, K. Kubo, T. Sakurai, Electron transfer-initiated photocyclization of substituted *N*-acetyl- α -dehydro(1-naphthyl)alanines to 1,2-dihydrobenzo[*f*]quinolinone derivatives: Scope and limitations, *Tetrahedron* 57 (2001) 5515–5526.
- [36] M. Bhalla, P.K. Naithani, T.N. Bhalla, A.K. Saxena, K. Shanker, Novel imidazole congeners as antiinflammatory agents, *J. Indian Chem. Soc.* 69 (1992) 594–595.
- [37] V. Voliani, R. Bizzarri, R. Nifosi, S. Abbruzzetti, E. Grandi, C. Viappiani, F. Beltram, Cis-trans photoisomerization of fluorescent-protein chromophores, *J. Phys. Chem. B* 112 (2008) 10714–10722.
- [38] C. Nishimura, T. Yamaoka, M. Mizutani, K. Yamashita, T. Akera, T. Tanimoto, Purification and characterization of the recombinant human aldose reductase expressed in baculovirus system, *Biochim. Biophys. Acta.* 1078 (1991) 171–178.
- [39] C. La Motta, S. Sartini, S. Salemo, F. Simorini, S. Taliani, A.M. Marini, F. Da Settimo, L. Marinelli, V. Limongelli, E. Novellino, Acetic acid aldose reductase inhibitors bearing a five-membered heterocyclic core with potent topical activity in a visual impairment rat model, *J. Med. Chem.* 51 (2008) 3182–3193.
- [40] R. Saito, M. Tokita, K. Uda, C. Ishikawa, M. Satoh, Synthesis and in vitro evaluation of botryllazine b analogues as a new class of inhibitor against human aldose reductase, *Tetrahedron* 65 (2009) 3019–3026.
- [41] A. Del Corso, L. Costantino, G. Rastelli, F. Buono, U. Mura, Aldose reductase does catalyse the reduction of glyceraldehyde through a stoichiometric oxidation of nadph, *Exp. Eye Res.* 71 (2000) 515–521.
- [42] R.P. Verma, Cytotoxicity of heterocyclic compounds against various cancer cells: A quantitative structure–activity relationship study, *Top. Heterocycl. Chem.* 9 (2007) 53–86.

- [43] C. Hansch, A. Leo, D.H. Hoekman, Exploring qsar: Fundamentals and applications in chemistry and biology, American Chemical Society, 1995.
- [44] K. Kato, K. Nakayama, M. Mizota, I. Miwa, J. Okuda, Properties of novel aldose reductase inhibitors, M16209 and M16287, in comparison with known inhibitors, ONO-2235 and sorbinil, Chem. Pharm. Bull. 39 (1991) 1540–1545.
- [45] U. Dhagat, S. Endo, A. Hara, O. El-Kabbani, Inhibition of 3(17) α -hydroxysteroid dehydrogenase (AKR1C21) by aldose reductase inhibitors, Bioorg. Med. Chem. 16 (2008) 3245–3254.
- [46] R.F. Rekker, The hydrophobic fragmental constant. Its derivation and application: A means of characterizing membrane systems, Elsevier Scientific Pub. Co.: distributors for the U.S. and Canada, Elsevier/North Holland, Amsterdam; New York, 1977.
- [47] C.A. Sotriffer, O. Kramer, G. Klebe, Probing flexibility and "induced-fit" phenomena in aldose reductase by comparative crystal structure analysis and molecular dynamics simulations, Proteins 56 (2004) 52–66.
- [48] H. Steuber, M. Zentgraf, C. La Motta, S. Sartini, A. Heine, G. Klebe, Evidence for a novel binding site conformer of aldose reductase in ligand-bound state, J. Mol. Biol. 369 (2007) 186–197.
- [49] R. Maccari, R. Ottanà, R. Ciurleo, M.G. Vigorita, D. Rakowitz, T. Steindl, T. Langer, Evaluation of in vitro aldose reductase inhibitory activity of 5-arylidene-2,4-thiazolidinediones, Bioorg. Med. Chem. Lett. 17 (2007) 3886–3893.
- [50] X. Chen, C. Zhu, F. Guo, X. Qiu, Y. Yang, S. Zhang, M. He, S. Parveen, C. Jing, Y. Li, B. Ma, Acetic acid derivatives of 3,4-dihydro-2H-1,2,4-benzothiadiazine 1,1-dioxide as a novel class of potent aldose reductase inhibitors, J. Med. Chem. 53 (2010) 8330–8344.
- [51] L. Zhang, H. Zhang, Y. Zhao, Z. Li, S. Chen, J. Zhai, Y. Chen, W. Xie, Z. Wang, Q. Li, X. Zheng, X. Hu, Inhibitor selectivity between aldo–keto reductase superfamily members AKR1B10 and AKR1B1: Role of Trp112 (Trp111), Febs Lett. 587 (2013) 3681–3686.
- [52] A. Cousido-Siah, F.X. Ruiz, A. Mitschler, S. Porte, A.R. de Lera, M.J. Martin, S. Manzanaro, J.A. de la Fuente, F. Terwesten, M. Betz, G. Klebe, J. Farres, X. Pares, A. Podjarny, Identification of a novel polyfluorinated compound as a lead to inhibit the human enzymes aldose reductase and akr1b10: Structure determination of both ternary complexes and implications for drug design, Acta Crystallogr D 70 (2014) 889–903.
- [53] J.J.P. Stewart, Optimization of parameters for semiempirical methods vi: More modifications to the nndo approximations and re-optimization of parameters, J. Mol. Model. 19 (2013) 1–32.
- [54] A. Klamt, G. Schuurmann, Cosmo: A new approach to dielectric screening in solvents with explicit expressions for the screening energy and its gradient, J. Chem. Soc., Perkin Trans. 2 (1993) 799–805.
- [55] R. Saito, T. Hirano, S. Maki, H. Niwa, Synthesis and chemiluminescent properties of 6,8-diaryl-2-methylimidazo[1,2- α]pyrazin-3(7H)-ones: Systematic investigation of substituent effect at *para*-position of phenyl group at 8-position, J. Photochem. Photobiol. A-Chem. 293 (2014) 12–25.
- [56] M.W. Schmidt, K.K. Baldrige, J.A. Boatz, S.T. Elbert, M.S. Gordon, J.H. Jensen, S. Koseki, N. Matsunaga, K.A. Nguyen, S.J. Su, T.L. Windus, M. Dupuis, J.A. Montgomery, General atomic and molecular electronic-structure system, J. Comput. Chem. 14 (1993) 1347–1363.
- [57] F. Jensen, Introduction to computational chemistry, 2nd ed., John Wiley and Sons, Ltd., West Sussex, UK, 2007.
- [58] C.T. Lee, W.T. Yang, R.G. Parr, Development of the colle-salvetti correlation-energy formula into a functional of the electron-density, Phys. Rev. B 37 (1988) 785–789.
- [59] A.D. Becke, Density-functional thermochemistry. 3. The role of exact exchange, J. Chem. Phys. 98 (1993) 5648–5652.
- [60] P.J. Stephens, F.J. Devlin, C.F. Chabalowski, M.J. Frisch, *Ab-initio* calculation of vibrational absorption and circular-dichroism spectra using density functional force fields, J. Phys. Chem. 98 (1994)

- [61] R. Hertwig, W. Koch, On the parameterization of the local correlation functional. What is Becke-3-LYP?, *Chem. Phys. Lett.* 268 (1997) 345–351.
- [62] Gold Version 5.2; The Cambridge Crystallographic Data Centre (CCDC): Cambridge, UK. <http://www.ccdc.cam.ac.uk>.
- [63] M.L. Verdonk, J.C. Cole, M.J. Hartshorn, C.W. Murray, R.D. Taylor, Improved protein–ligand docking using gold, *Proteins* 52 (2003) 609–623.
- [64] O. Korb, T. Stütze, T.E. Exner, Empirical scoring functions for advanced protein-ligand docking with plants, *J. Chem. Inf. Model.* 49 (2009) 84–96.
- [65] W.T.M. Mooij, M.L. Verdonk, General and targeted statistical potentials for protein-ligand interactions, *Proteins* 61 (2005) 272–287.
- [66] Cambridge Crystallographic Data Centre, Gold scoring function performance against the dud decoy/active set. https://www.ccdc.cam.ac.uk/support-and-resources/ccdcresources/Vs_workcase.pdf, 2012 (14.09.16).
- [67] Discovery studio visualizer Release 4.1; Dassault Systèmes BIOVIA: San Diego, USA. <http://accelrys.com/products/collaborative-science/biovia-discovery-studio/visualization.html>.
- [68] M.L. Verdonk, J.C. Cole, R. Taylor, Superstar: A knowledge-based approach for identifying interaction sites in proteins, *J. Mol. Biol.* 289 (1999) 1093–1108.
- [69] M.L. Verdonk, J.C. Cole, P. Watson, V. Gillet, P. Willett, Superstar: Improved knowledge-based interaction fields for protein binding sites1, *J. Mol. Biol.* 307 (2001) 841–859.
- [70] D.R. Boer, J. Kroon, J.C. Cole, B. Smith, M.L. Verdonk, Superstar: Comparison of csd and pdb-based interaction fields as a basis for the prediction of protein-ligand interactions1, *J. Mol. Biol.* 312 (2001) 275–287.
- [71] L.K. Soni, S.G. Kaskhedikar, Exploring structural requirements for aldose-reductase inhibition by 2,4-dioxo-5-(naphth-2-ylmethylene)-3-thiazolidinyl acetic acids and 2-thioxo analogues: Fujita-ban and hansch approach, *Arch. Pharm.* 339 (2006) 327–331.
- [72] C. Nantasenamat, T. Monnor, A. Worachartcheewan, P. Mandi, C. Isarankura-Na-Ayudhya, V. Prachayasittikul, Predictive qsar modeling of aldose reductase inhibitors using monte carlo feature selection, *Eur. J. Med. Chem.* 76 (2014) 352–359.
- [73] M. Zentgraf, H. Steuber, C. Koch, C. La Motta, S. Sartini, C.A. Sotriffer, G. Klebe, How reliable are current docking approaches for structure-based drug design? Lessons from aldose reductase, *Angew. Chem. Int. Ed.* 46 (2007) 3575–3578.
- [74] S.V. Jain, K.S. Bhadoriya, S.B. Bari, Qsar and flexible docking studies of some aldose reductase inhibitors obtained from natural origin, *Med. Chem. Res.* 21 (2012) 1665–1676.

Figure 1



Scheme 1

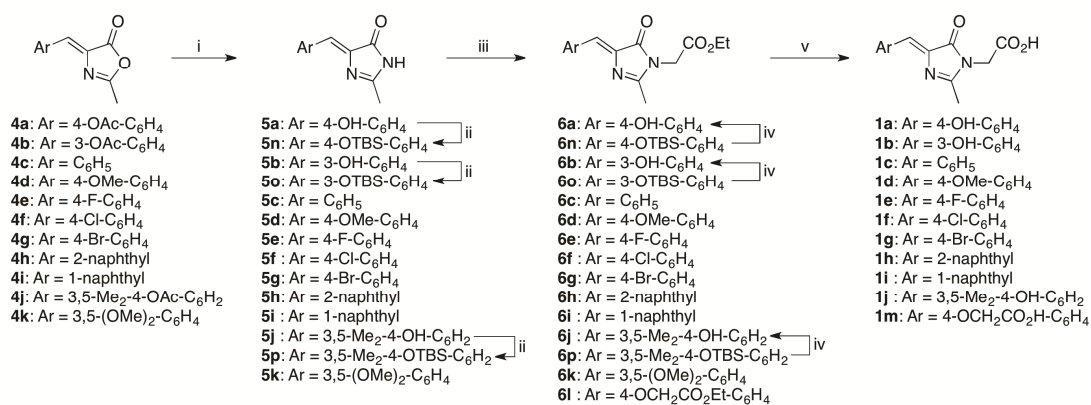
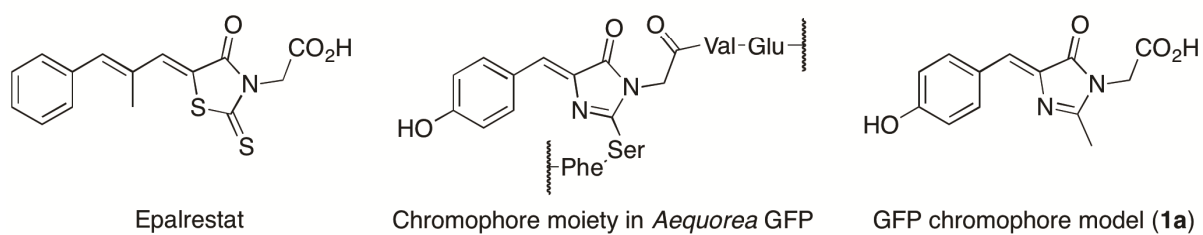
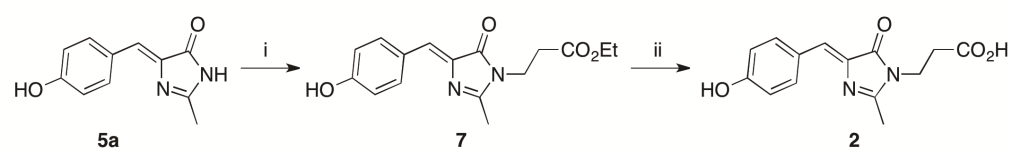
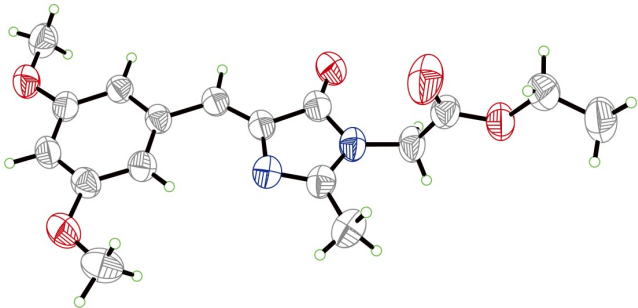


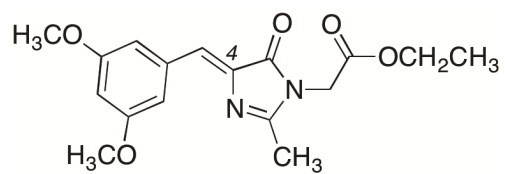
Figure 2. Structures of epalrestat, the chromophore moiety in the *Aequorea* green fluorescent protein (GFP), and the GFP chromophore model compound **1a**.



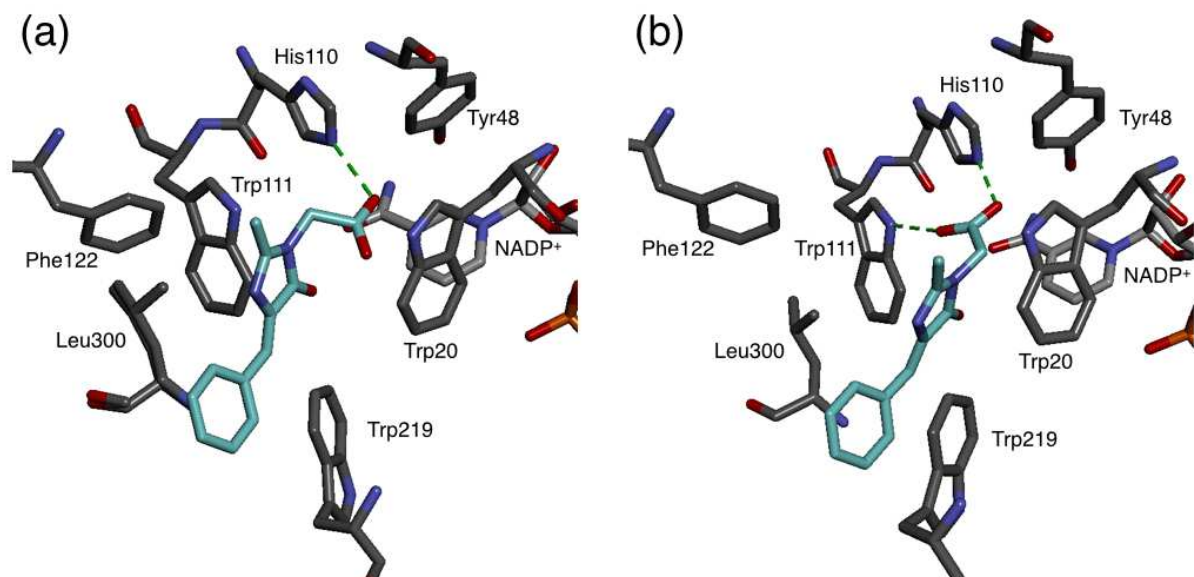
Scheme 2

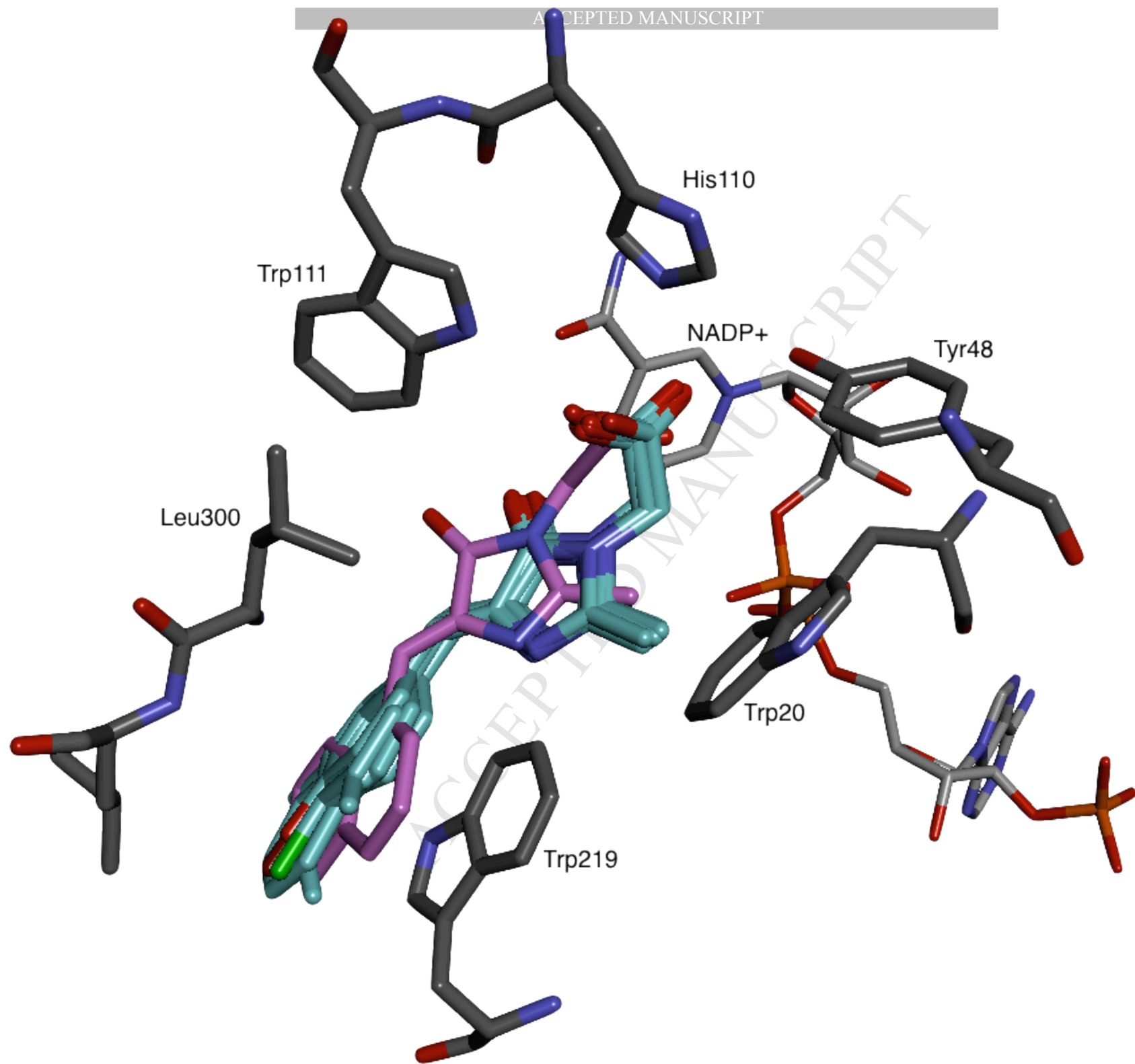


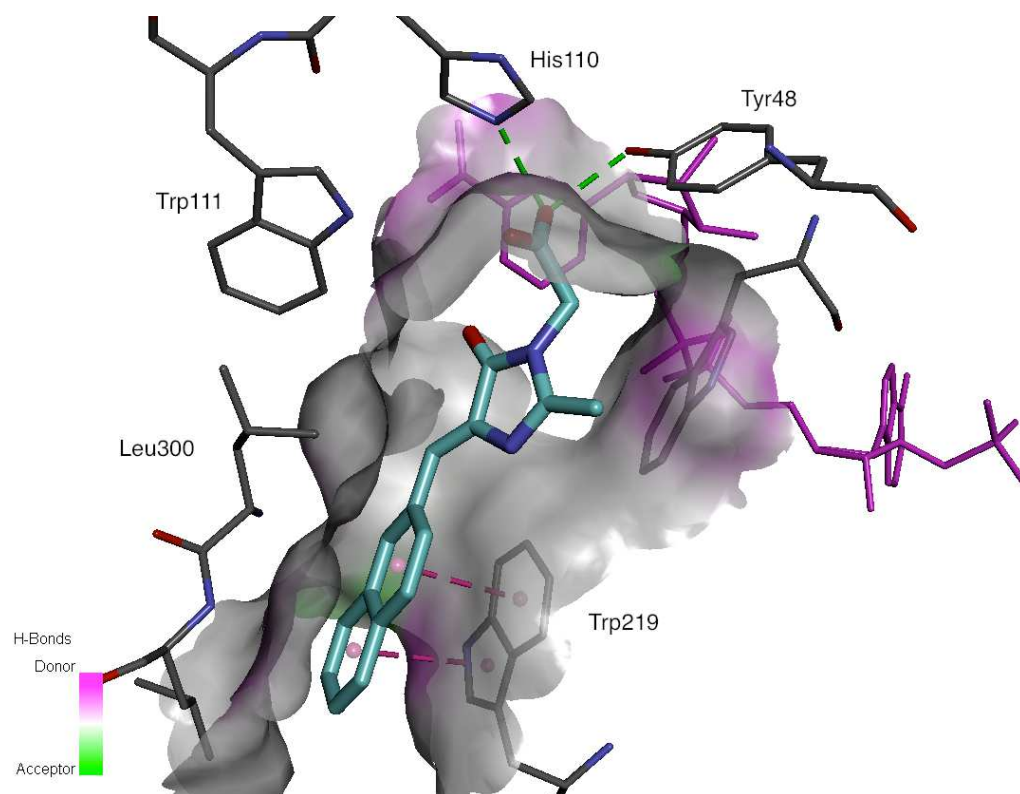


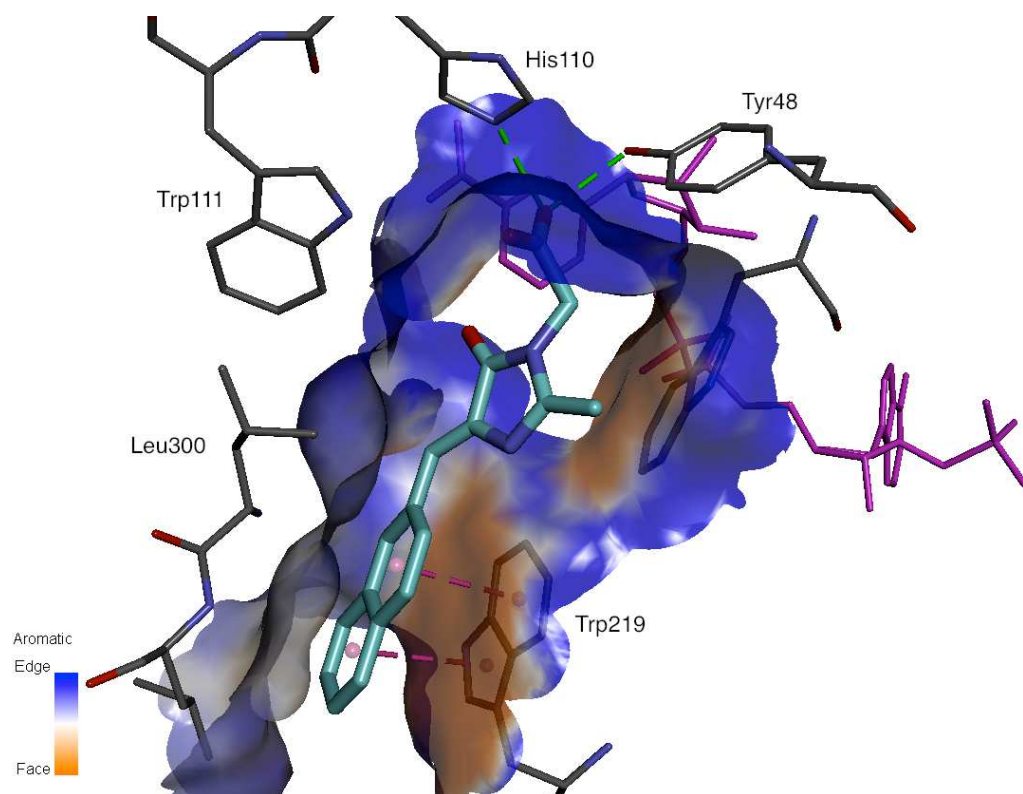


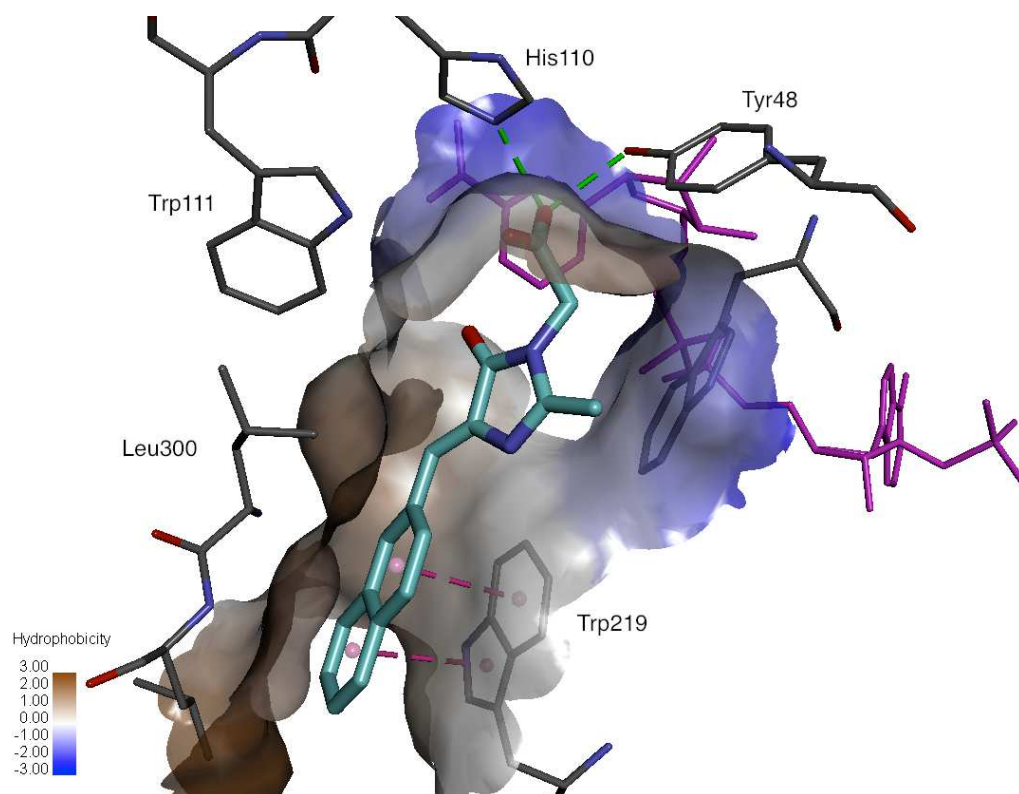
ACCEPTED MANUSCRIPT

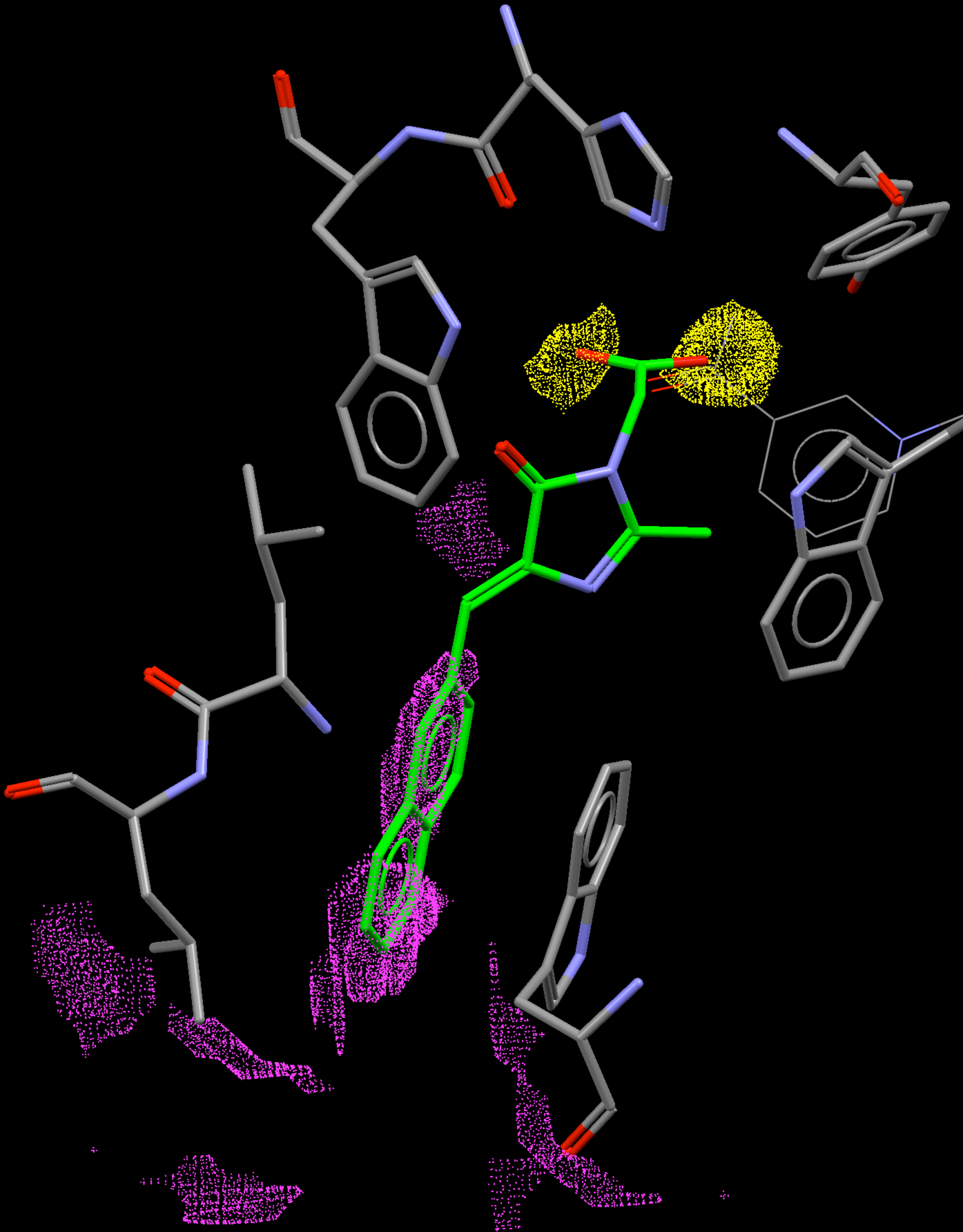


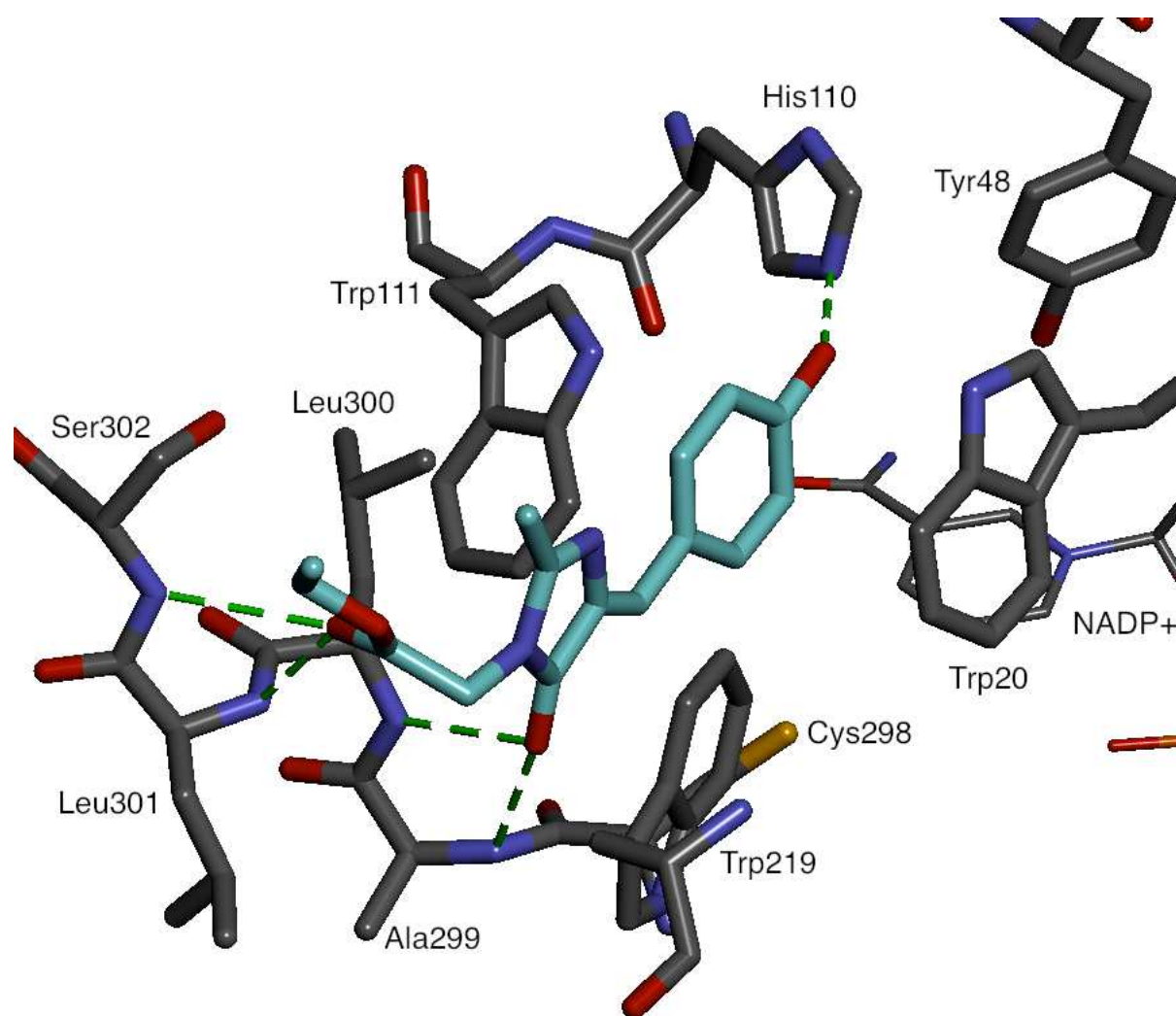




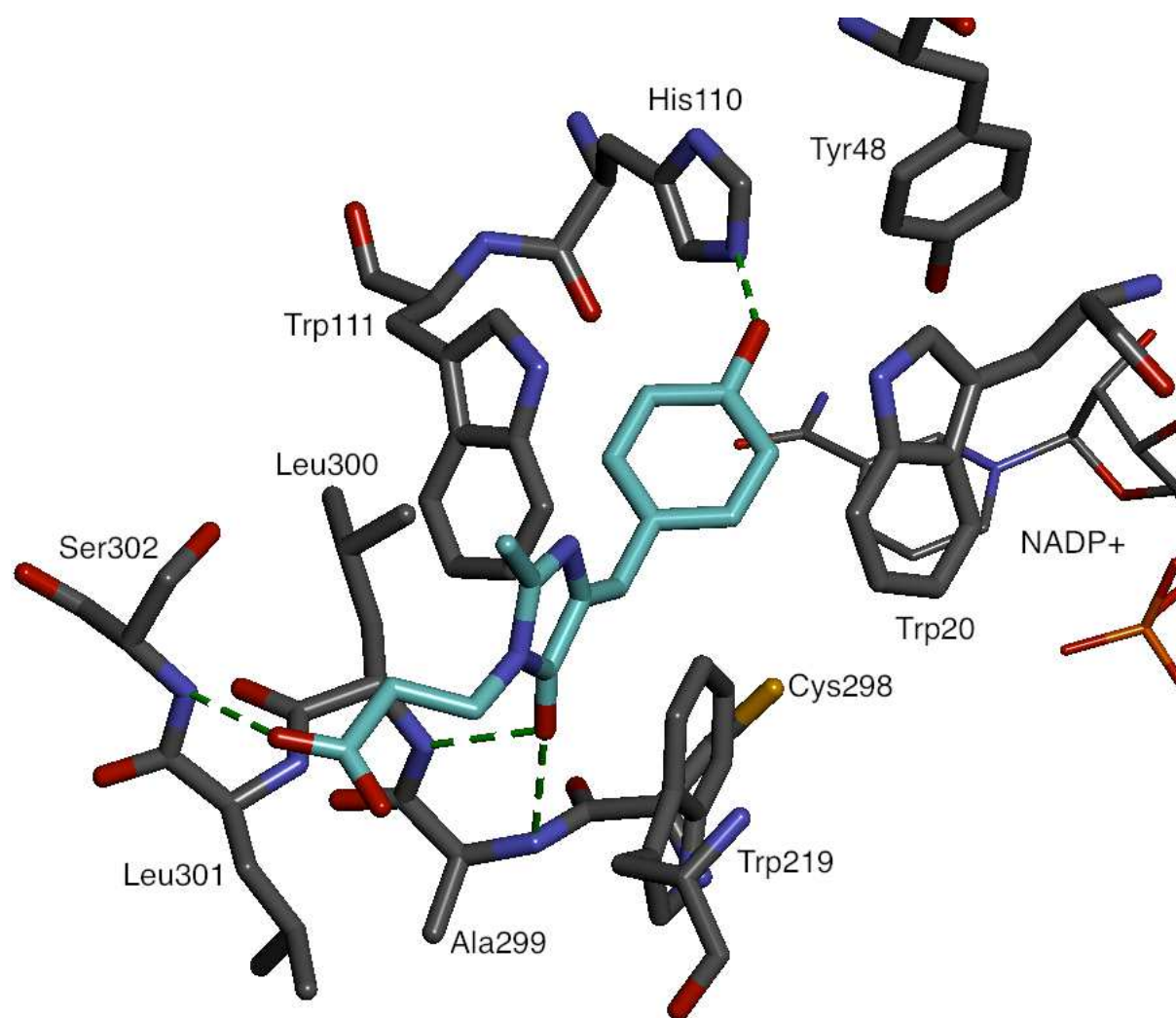


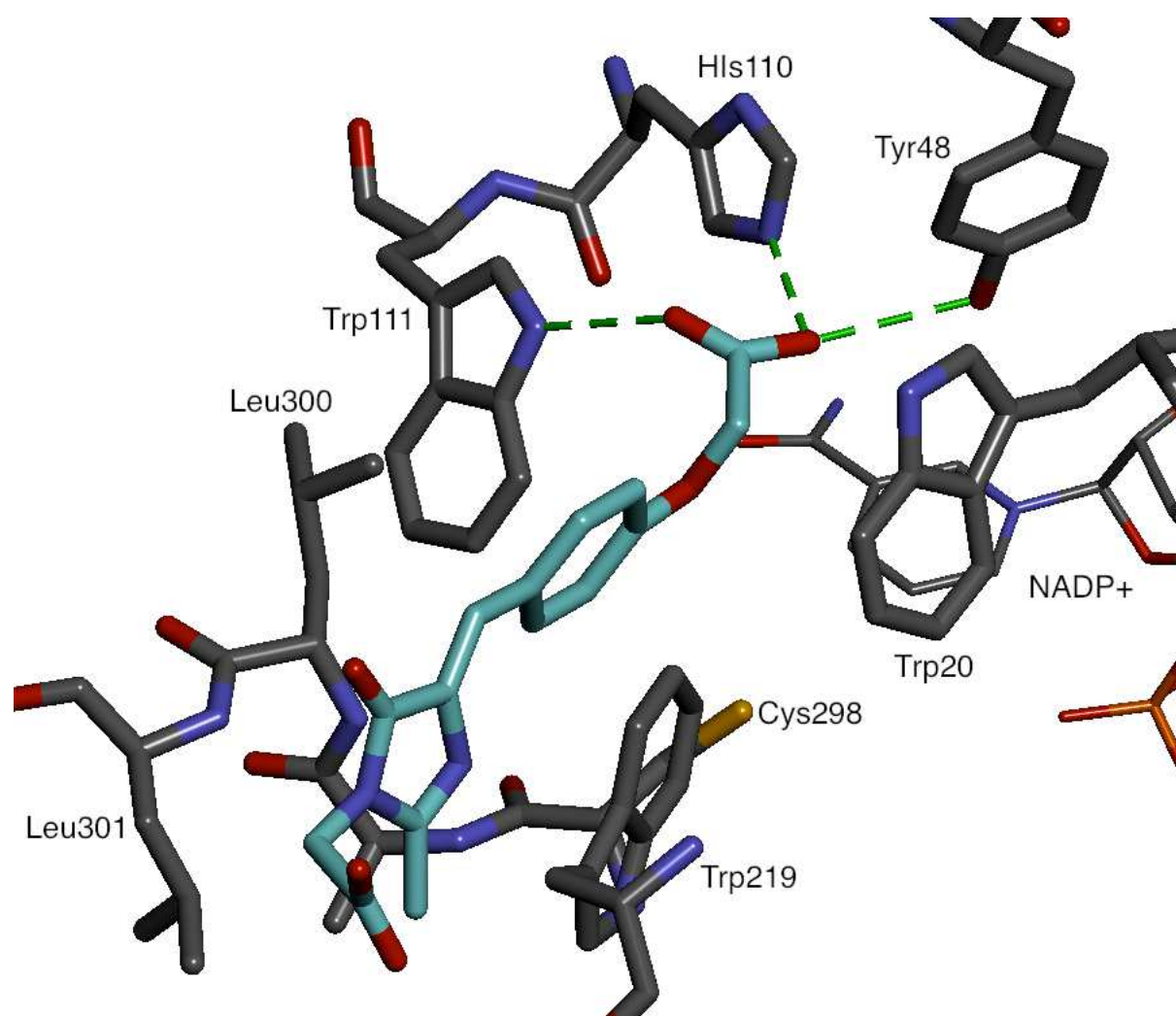


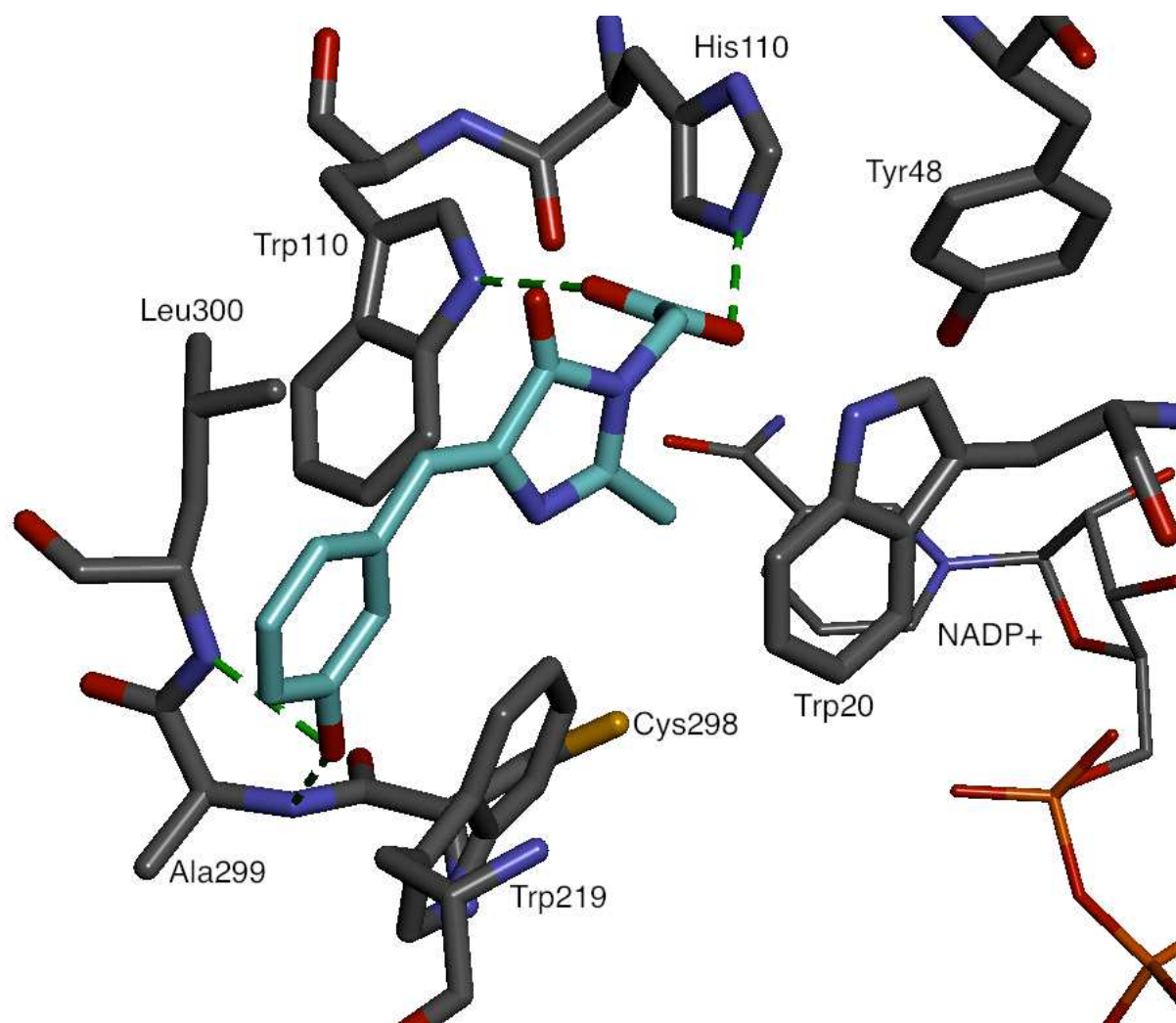




ACCEPTED







ACCEPTED

Green fluorescent protein chromophore derivatives as a new class of aldose reductase inhibitorsRyota Saito,^{a,b*} Maiko Hoshi,^a Akihiro Kato,^a Chikako Ishikawa,^c and Toshiya Komatsu^d^aDepartment of Chemistry, Toho University, 2-2-1 Miyama, Funabashi, Chiba, 274-8510 Japan;^bResearch Center for Materials with Integrated Properties, Toho University, 2-2-1 Miyama, Funabashi, Chiba 274-8510, Japan; ^cFaculty of Pharmaceutical Science, Toho University, 2-2-1 Miyama, Funabashi, Chiba, 274-8510 Japan; ^dKowa Company, Ltd., 3-4-14 Nihonbashi-honcho, Chuo-ku, Tokyo 103-8433, Japan**Highlights:**

- Some novel (*Z*)-4-arylmethylidene-1*H*-imidazol-5(4*H*)-ones were synthesized.
- **1h** showed equal activity to the only drug for diabetic complications in the market.
- This compound proved to be potential new drugs for diabetic complications.
- Correlation analyses between docking scores and actual IC₅₀ values were performed.
- This method was found to be useful for docking studies with induced-fit type enzymes.